



Article

Fourier Synchrosqueezing Transform-ICA-EMD Framework Based EOG-Biometric Sustainable and Continuous Authentication via Voluntary Eye Blinking Activities

Kutlucan Gorur

Electrical and Electronics Engineering Department, Bandırma Onyedi Eylül University, 10250 Balıkesir, Turkey; kgorur@bandirma.edu.tr

Abstract: In recent years, limited works on EOG (electrooculography)-based biometric authentication systems have been carried out with eye movements or eye blinking activities in the current literature. EOGs have permanent and unique traits that can separate one individual from another. In this work, we have investigated FSST (Fourier Synchrosqueezing Transform)-ICA (Independent Component Analysis)-EMD (Empirical Mode Decomposition) robust framework-based EOG-biometric authentication (*one-versus-others* verification) performances using ensembled RNN (Recurrent Neural Network) deep models voluntary eye blinkings movements. FSST is implemented to provide accurate and dense temporal-spatial properties of EOGs on the state-of-the-art time-frequency matrix. ICA is a powerful statistical tool to decompose multiple recording electrodes. Finally, EMD is deployed to isolate EOG signals from the EEGs collected from the scalp. As our best knowledge, this is the first research attempt to explore the success of the FSST-ICA-EMD framework on EOG-biometric authentication generated via voluntary eye blinking activities in the limited EOG-related biometric literature. According to the promising results, improved and high recognition accuracies (ACC/Accuracy: $\geq 99.99\%$ and AUC/Area under the Curve: 0.99) have been achieved in addition to the high TAR (true acceptance rate) scores ($\geq 98\%$) and low FAR (false acceptance rate) scores ($\leq 3.33\%$) in seven individuals. On the other hand, authentication and monitoring for online users/students are becoming essential and important tasks due to the increase of the digital world (e-learning, e-banking, or e-government systems) and the COVID-19 pandemic. Especially in order to ensure reliable access, a highly scalable and affordable approach for authenticating the examinee without cheating or monitoring high-data-size video streaming is required in e-learning platforms and online education strategies. Hence, this work may present an approach that offers a sustainable, continuous, and reliable EOG-biometric authentication of digital applications, including e-learning platforms for users/students.

Keywords: EOG-biometric; FSST; ICA; EMD; ensembled RNN-deep models; E-learning



Citation: Gorur, K. Fourier Synchrosqueezing Transform-ICA-EMD Framework Based EOG-Biometric Sustainable and Continuous Authentication via Voluntary Eye Blinking Activities. *Biomimetics* **2023**, *8*, 378. <https://doi.org/10.3390/biomimetics8040378>

Academic Editor: Stanislav N. Gorb

Received: 20 July 2023

Revised: 8 August 2023

Accepted: 11 August 2023

Published: 18 August 2023



Copyright: © 2023 by the author. Licensee MDPI, Basel, Switzerland. This article is an open access article distributed under the terms and conditions of the Creative Commons Attribution (CC BY) license (<https://creativecommons.org/licenses/by/4.0/>).

1. Introduction

Physiological and behavioral biometric traits can separate one individual from another and deal with identifying and verifying a unique person. These traits can be permanent, unique, and complex definitional in biometric authentication systems. The systems observe the security aspects of the applications that are imperative for security requirements of the digital world and technologies [1,2]. Biometric authentication systems have been steadily growing in popularity due to the development of many useful, challenging, and widely accepted applications, such as security issues and identity access management, such as cellphones, laptops, and entering a building [3,4]. These systems offer approaches to solve access control problems related to the authentication and verification stages [1,2,5].

Biometric authentication techniques implement behavioral or physiological features, including fingerprint, palm print, face pattern, iris, voice, and gait analysis to identify

someone [6,7]. Physiological traits are known as the physical traits of an individual (fingerprint and hand etc.), and these static attributes are widely accepted because of their collectability and inexpensive characteristics in verification [1]. However, these static conventional biometric methods can be abused and sometimes can be easily accessed by imposters attacks [8,9]. Hence, security concerns against threats and fraud exist in these biometric approaches. On the other hand, in recent years, dynamic biological biometric traits are gaining popularity using EEG (electroencephalography), ECG (electrocardiogram), EMG (electromyogram), and PPG (photoplethysmography) signals [2,8,10]. All these 1D time-series signals have advantages and disadvantages in authentication systems. For example, lately, electroencephalography (EEG)-based authentication has received considerable attention from the scientific community. However, the limited usability of these biometric systems has been noted due to the high mental effort and continuous requirement of cognitive ability (hard-to-elicited motor imagery EEGs) [11]. ECG-based biometry will also succeed if fiducial points (P, QRS, and T complexes) are correctly identified in intrabeat and interbeat variations. However, correctly identifying fiducial points is reported as a difficult task in a practical biometric application scenario [8].

Electrooculography (EOG) is electrical activity resulting from a potential change due to eyeball or eyelid movements. The EOG waveform is recorded with skin electrodes around the eyes, or EEG electrodes are placed on the scalp. The amplitude of the EOG signals occurs between 10 and 200 μV and has been observed to change at frequencies falling within the 0.5–15 Hz range. The eyeball acts as a dipole and charged organ [12–14]. The positive and negative poles are oriented anteriorly (cornea) and posteriorly (retina). When the eyeball rotates about its axis, thus acting can generate a detectable amplitude electric signal that is distinguished by any electrodes near the eye or scalp electrodes. When the eyeball rotates upwards, the positive pole (cornea) closes to the frontal electrodes, producing positive deflection changes. Otherwise, when the eyeball rotates downwards (closer to the ear reference electrodes), it produces a negative deflection change. Deflections of eye blink resemble this situation. When the eyelid closes, the cornea closes to frontal electrodes, and a positive pulse occurs. However, the eyelid opens, and the cornea rotates away from the frontal electrodes, producing a negative pulse. The duration of eye blinking occurs in the range of 300 to 400 ms [14].

The proposed authentication process with FSST-ICA-EMD framework and voluntary eye blinking activity employs convenient methods (such as *one-versus-others* strategy and template matching) to confirm identity in the enrollment and authentication phases. In order to accomplish this, the following technical contributions were made:

- This article proposes a *one-versus-others* biometric authentication approach investigating FSST-ICA-EMD framework using ensembled Recurrent Neural Network (RNN) models via voluntary eye blinking activities (EOG responses) to high correct recognition rates, reliable and suitable for next-generation consumer electronic devices. According to our best knowledge, this is the first attempt to explore high-level time-frequency features extracted by FSST and decomposed EOGs via ICA and EMD in a combined framework for EOG-biometric authentication in the existing literature.
- Verifying the proposed authentication approach is essential via statistical discrimination to present a robust and effective system. Hence, this work is a first attempt to implement broad statistical methods to estimate discrimination EOG-biometric besides the correction rates (sensitivity, F-score, accuracy etc.) and TAR/FAR score metrics.
- Visualizing the functional brain connectivity with circular graphs and brain mappings during eye-blinking activity. The following key superiority the FSST-ICA-EMD framework for EOG-biometric authentication focuses on the short-length of time (only 0.5 s) for training/testing/attempt processes for deep RNN models in enrollment and authentication. As far as we know, this time-segment is the least for the mentioned processes of the deep models. Thus, this advantage might address some of the afore-

mentioned problems for swift enrollment and authentication phases [8]. The most used terms in the article are listed in Table 1.

Table 1. The list of abbreviations in the paper.

Abbreviations	Descriptions
EOG	Electrooculography
FSST	Fourier Synchrosqueezing Transform
ICA	Independent Component Analysis
EMD	Empirical Mode Decomposition
RNN	Recurrent Neural Network
LSTM	Long Short Term Memory
BiSLTM	Bidirectional LSTM
GRU	Gated Recurrent Unit
EEG	Electroencephalography
EMG	Electromyogram
EKG	Electrocardiogram
TAR	True Acceptance Rate
FAR	False Acceptance Rate

The article is also organized as well: Section 2 discusses the literature review for this work. Section 3 addresses the methods and dataset descriptions. The results section is explained in Section 4. Section 5 reports the conclusion section to analyze outcomes and future work.

2. Literature Review

In recent years, the capability of eye-blinking EOG (electrooculogram) signals has been explored to discriminate between individuals in EOG-based biometric authentication systems. The eye-blinking EOG signals are extracted from brain waves recorded using an EEG headset. This new modality for authentication is a promising method. Furthermore, it has achieved a high recognition rate of up to >90.0% in identification mode and a low false acceptance rate (FAR) among multiple persons [12]. Moreover, a multi-level EEG-based authentication approach with EOG signals has also been reported in the limited literature [13,14]. Jalilifard et al. have developed a hybrid human authentication system using EEG and EOG signals generated by involuntary spontaneous blinking eye movements. Patterns of a series of blinks were processed by using Gated Recurrent Unit (GRU), and the classification accuracy was obtained over >98.0% [14]. In another study, Abo-Zahhad et al. provided a human recognition system voluntary eye-blinking waveform of around 97.0% in the test phase of identification mode. Linear Discriminant Analysis (LDA) was implemented to identify 25 individuals [15]. Juhola et al. has proposed a hybrid biometric system with EOG and VOG (video-oculography) signals using shallow machine learning models (kNN, LDA, etc.). This verification method employs saccadic eye movements to reliably distinguish a legitimate person from others in the range of 45–99% correct recognition rates [15]. Empirical Mode Decomposition (EMD) was applied to isolate EOGs from raw EEG signals using the decomposition process into Intrinsic Mode Functions (IMFs) [12,14].

In addition, eye blink features have also been implemented several other image and video-based research. Eye movement features (the motion, speed, energy, and frequency signal of eye blinks) were reported consisting of implicit and dynamic patterns that occurred on the microsecond temporal resolution of event densities [16]. Hence, these studies were offered to be used in eye-tracking applications [16]. The disadvantage of this kind of work, participants/students have to look at the monitor or camera consistently during the authentication process [17]. Especially this progress is a hard task for students in online e-learning/e-assessment education and it needs a high-speed internet [17]. In recent times after the COVID-19 pandemic, the need for sustainable and continuous online monitoring and authentication to e-learning platforms has evolved to seek accurate identification and verification for performing any behavior not authorized by the device on which students

perform the activity [17–29]. Thanks to these important opportunities of biosignal-based authentication ways, e-learning platform courses/examinations may be provided as an effective verification in the learning-teaching experience [18]. Thus it might be widely accepted in all educational environments as a different alternative to traditional monitoring systems. In the limited literature on e-learning and authentication, most works concern monitoring technologies (webcams and microphones). However, according to our best knowledge, there is a lack of study implementation of EOG-biometric authentication technology as sustainable and continuous access for e-learning platforms. Digital Transformation (DT) must be adapted to competitive strategies and constantly renewed to succeed in the global competition of education and economics. The most significant of these innovations is secure access to the DT. Thus the strategic significance of different biometric authentication in today's global education and a sustainable environment will be anticipated in growing cases day by day. Furthermore, short-time enrollment/authentication phases during secure and quick access to the digital e-learning platforms can also concentrate on the economic situation of "Sustainable Energy" [19].

This study aims to develop Fourier Synchrosqueezing Transform (FSST)-ICA-EMD framework-based EOG-biometric authentication approach using voluntary eye blinkings. The Fourier SST proposes a sharper time-frequency estimation by reconstruction of the coefficients for the time-frequency matrix [30]. The relevant time-series features are extracted by the Fourier SST (FSST), and this time-frequency representation can provide better performance for the detection of patterns in biosignals [31,32]. Independent Component Analysis (ICA) employs statistical technique background to decompose mixed multi-channel sources into statistically independent channels [33]. This technique decomposes each multi-channel recorded EEG/EOG signal set into temporally independent components [34]. Here, the ICA was the fundamental method to provide high true acceptance rate (TAR) and low false acceptance rate (FAR) metrics in multiple times attempts to the ensemble (Long Short Term Memory) models for EOG-biometric *one-versus-others* authentication. In addition, EMD was used to extract EOGs from the raw EEG signals to explore the accuracy and other performance metrics regarding the isolated eye-blinking waveforms [14].

3. Methods and Materials

3.1. Related Work and Motivation

This article proposes a robust and effective EOG-biometric authentication approach using voluntary eye blinking movements consisting of enrollment and authentication phases (see Figure 1). These waveform biometric traits protect private information stored in digital devices. The unique primary novelty of the processing of EOG signals is based on the FSST-ICA-EMD framework. Fourier SST can prompt high-resolution time-frequency feature extraction for time-series data [32]. On the other hand, ICA separates statistically independent components for multichannel recordings, and EMD is able to isolate EOG signals from EEGs [15,33]. The combined framework has highly capable of reliable and high-performance *one-versus-others* EOG-biometric authentication implementing ensembled RNN models. Majority voting, matching, and thresholding are also implemented to achieve consistent performance metrics. Time-segment generator extract random frames (0.5 s for 100 times) from the time-series data are to attempt these frames (for determining TAR and FAR scores) into the ensembled RNN models.

The applied statistical techniques in the work are:

- t-distributed stochastic neighbor embedding (t-SNE) was employed to demonstrate scattering for distinction.
- Probability density function (PDF) distribution for the distinction individuals (cross-subject and same-subject) over the diverse scalp parts.
- Correlation matrix for each subject to verify the unique pattern.
- Recurrence Plot (RP) is used for the separation of sequential recorded channel source separation to verify the ICA/EMD technique effectiveness.

- MANOVA (Multivariate ANOVA) analysis was to describe grouping separation among individuals.
- Functional connectivity analysis was drawn to correlate each brain cortices over the Circular Graph technique.

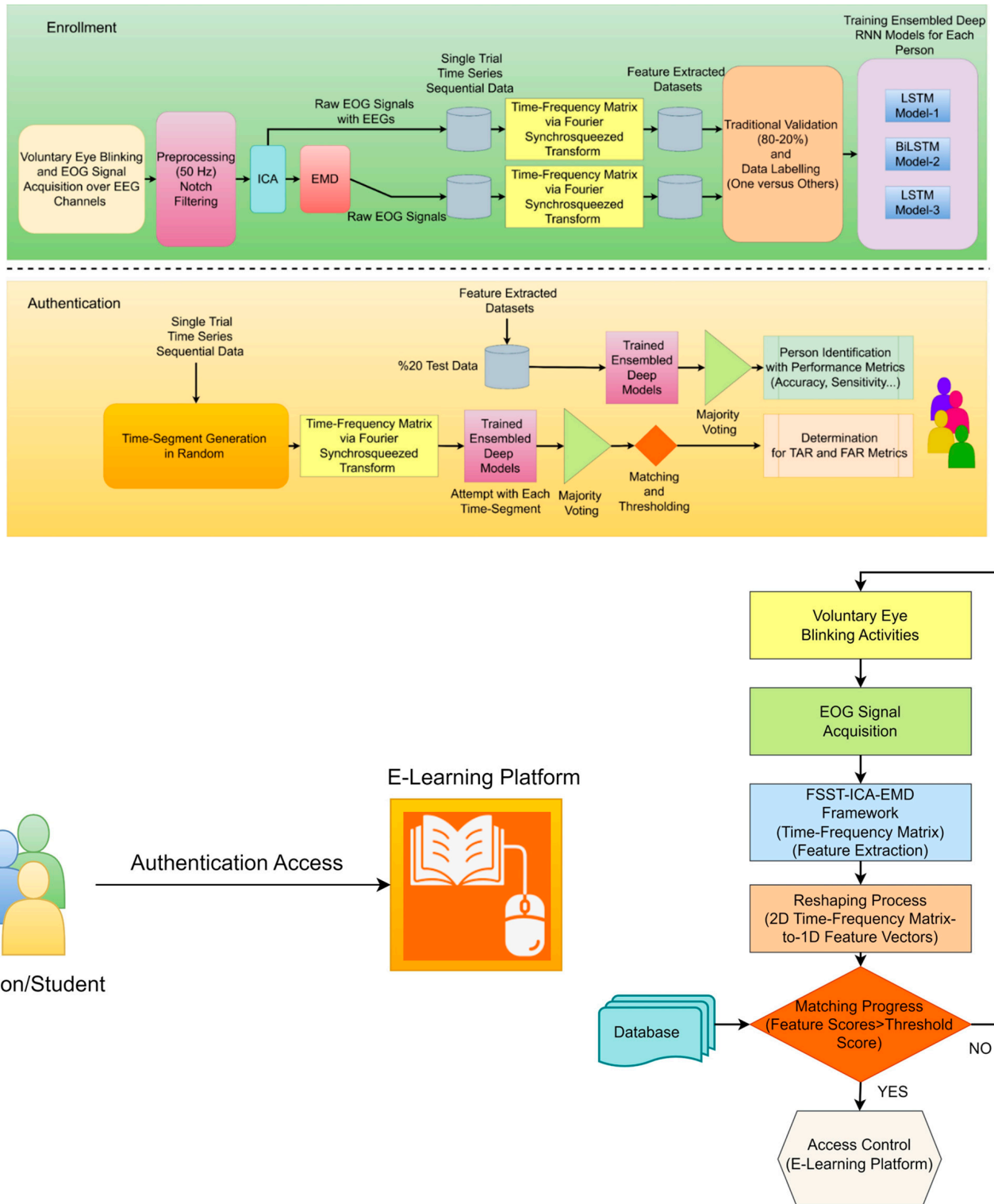


Figure 1. The scheme of FSST-ICA-EMD framework-based EOG-biometric authentication over voluntary eye blinkings/vertical saccades (**upper**), an approach for e-learning platform access and flow chart algorithm (**lower**).

3.2. Eye Blinking Activity and EOG Signal Acquisition

Eye blinking movement generated EOG responses (see Figure 2) were recorded in a noninvasive manner over the scalp with the Micromed SAM32RFO acquisition device. The impedance values were kept under the 10 kΩ. The sampling frequency was 1024 Hz and 50 Hz notch filter was applied to remove the power line noise [11]. After a filtering operation, the raw EOG signals are decomposed source separation via ICA and made extraction EOGs from brain activity via EMD according to the literature background (see Figure 1) [15,33]. The headset has 19 wet electrodes (see Table 2 for enumerated channels). The international 10–20 electrode placement system was employed with monopolar leads on the scalp (see Figure 3). Left-right earlobes (A1–A2) and left eyebrow are defined as the references and ground, respectively [11]. The indication of the brain cortex in the Figure 3 are titled as; F: Frontal, C: Central, T: Temporal, O: Occipital and P: Parietal.

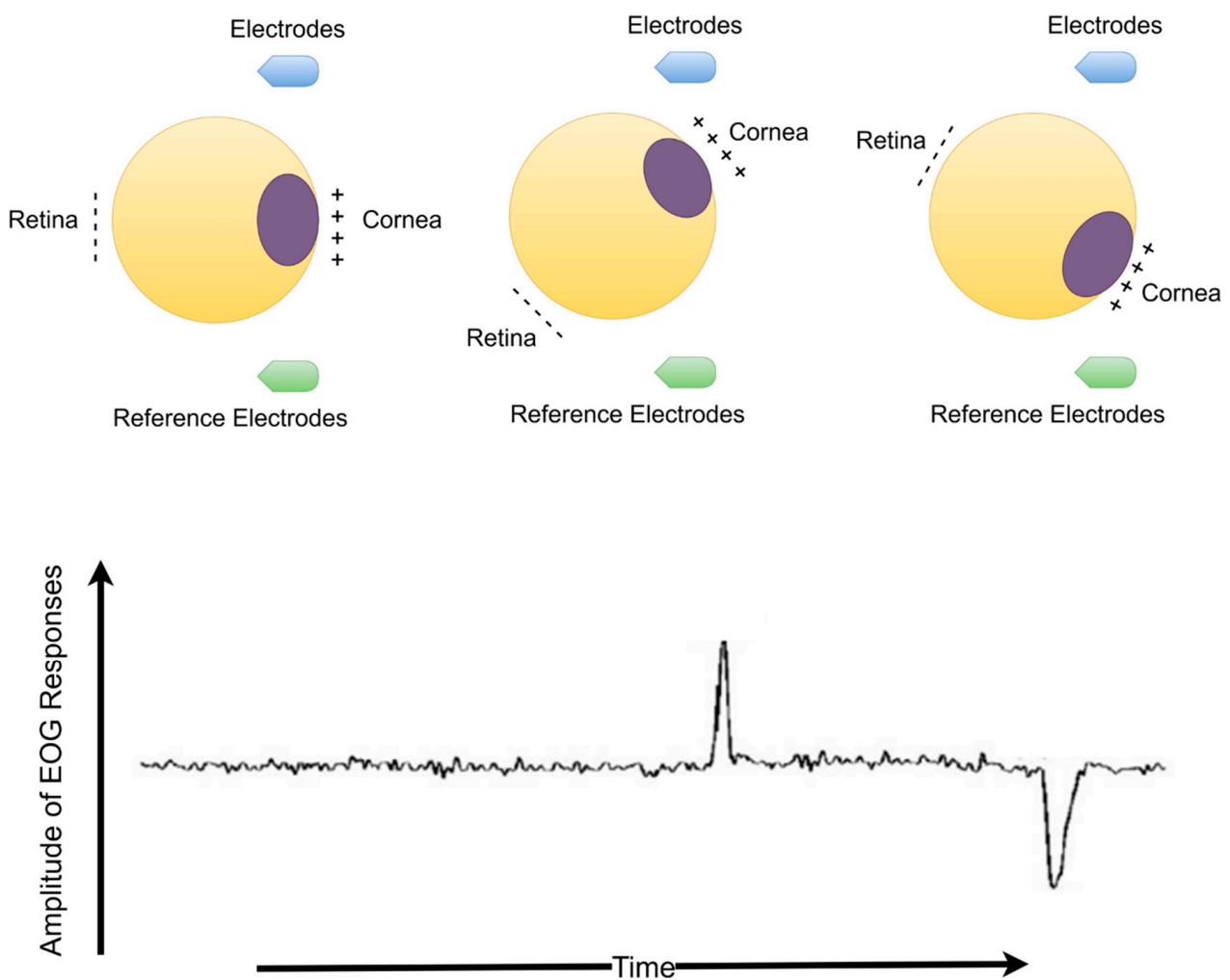


Figure 2. The dipole model of eyeball with EOG waveforms (Eye blinking waveforms during eyelid opening and closure have similar activity responses in terms of the generation).

Table 2. The monopolar placement list for EEG electrodes.

Ch. Num.	1	2	3	4	5	6	7	8	9	10	11	12	13	14	15	16	17	18	19
Ch. Name	Fp1	Fp2	F7	F3	Fz	F4	F8	T3	C3	Cz	C4	T4	T5	P3	Pz	P4	T6	O1	O2

Ch. Num: Channel Number, Ch. Name: Channel Name.

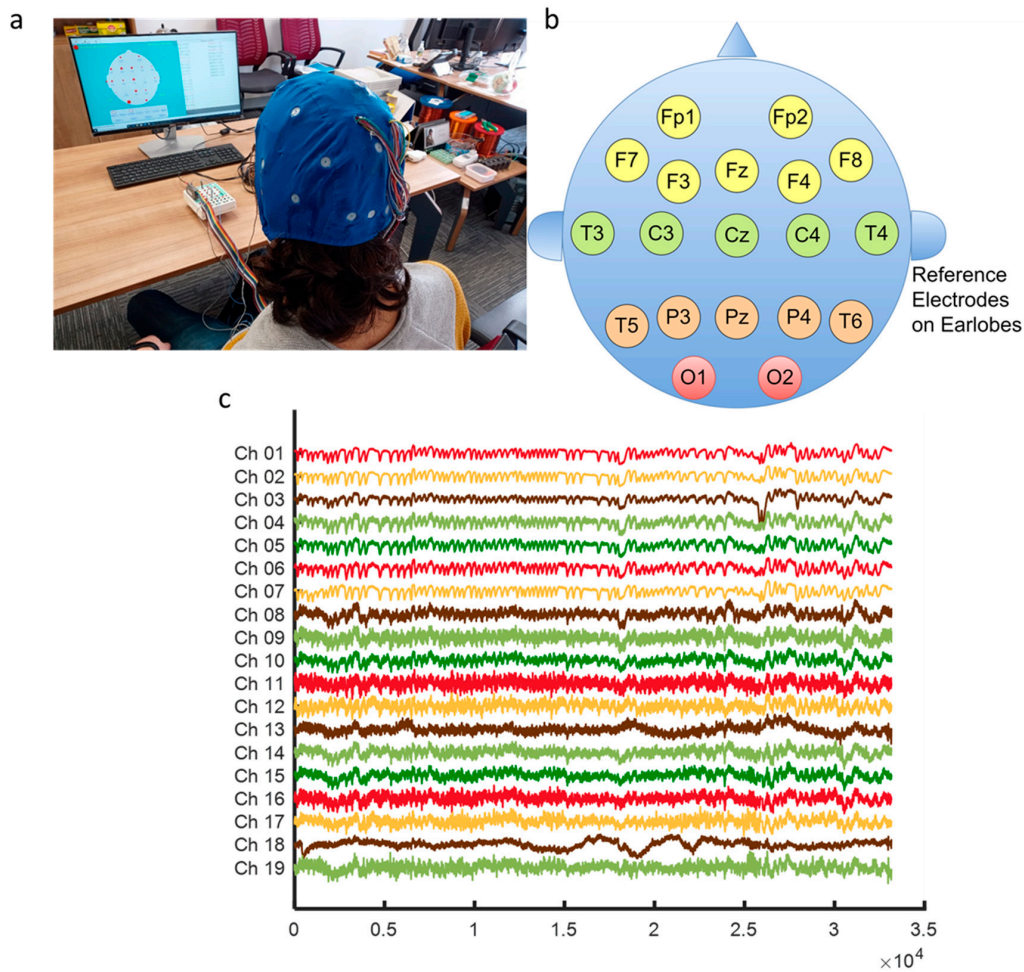


Figure 3. Signal acquiring scheme for EOG-biometric authentication with voluntary eye blinkings (a) Electrode placement setup on the scalp (b) Indication of brain lobe locations (c) Recorded EOG responses (from the Subject-5 samples).

3.3. Trial Organization

For this experiment, we settled on a single-trial organization consisting of multiple voluntary eye-blinking movements. The participants followed the experimental instructions on a monitor (17" LCD). These instructions are represented in Figure 4. Each experimental trial included different phases; starting point fixation, voluntary eye blinking movements, ready for relaxation, and resting state.

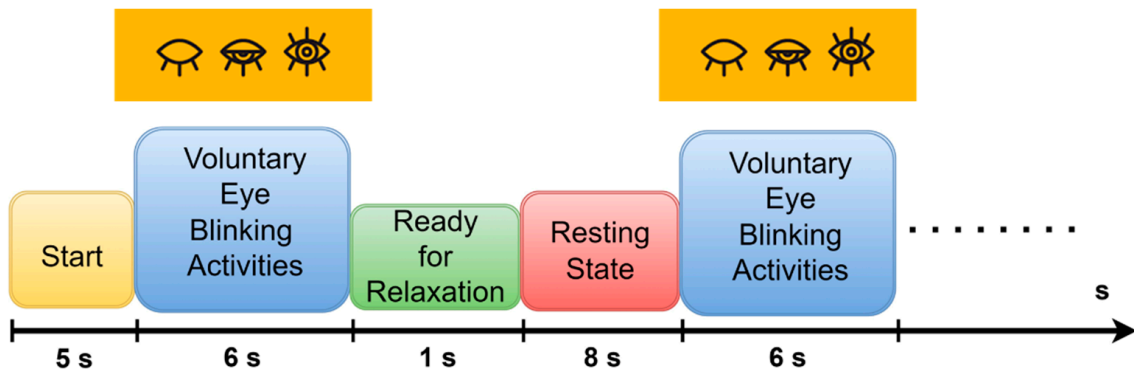


Figure 4. Experimental procedure for recording voluntary eye blinking activities in single-trial phases.

According to an experimental procedure, this trial organization begins with a start fixation point. Then the voluntary eye-blinking activities were carried out for 6 s without movement. After that, 1 s and 8 s periods are stated as the ready relaxation and resting state phases, respectively. The same process is repeated six times, and the entire trial is conducted, lasting 86 s duration. Therefore, the dataset size for eye blinking acting based EOGs is recorded as $36,864 \times 19$ ($6 \text{ s} \times 1024 \text{ sampling rate} \times 6 \text{ times} \times 19 \text{ channels}$) for each participant during a single trial. In the resting state phases, the participants were instructed to simultaneously think of hand-action motor imagery (EEGs). However, the resting state phases were cut out to define EOG activity solely in the developed EOG-biometric authentication.

Naive and healthy subjects (aged from 20 to 38) were recruited for this experiment, including students and academic staff at the Bandirma Onyedi Eylül University. One focus point is to explore the FSST-ICA-EMD framework with limited users in EOG-based authentication. Furthermore, male (3) and female (4) subject numbers were chosen in close proportions to prevent from gender bias. Reliably distinguishing legitimate student children with electrooculography is suitable in computational verification due to the easy-to-use and universal characteristic of eye blinking activities.

3.4. Time-Frequency Feature Extraction and Ensembled RNN Models

Feature extraction is reported as a critical step in developing effective and robust biometric systems. This Fourier Synchrosqueezing Transform (FSST)-based feature extraction strategy was proposed to extract time-frequency domain features for each time segment (0.5 s) of eye-blinking EOG signals. Then time-frequency matrices (based on FSST) were employed to enable ensembled RNN models for the one-versus-others biometric authentication systems. FSST reorganizes energy only in the frequency direction and is a highly effective way. Therefore, the time resolution of EOG signals can be effectively maintained in the time-frequency domain. As far as we know, in terms of the available literature background, this FSST-based feature extraction technique is used to improve EOG-biometric authentication performance for the first time in this research study. The time-frequency feature extraction process is shown in Figure 5.



Figure 5. Spectral feature engineering technique via FSST for temporal-spatial pattern.

Ensemble methods are a technique that combines predictions of various machine learning models, which helps classification models to have stronger generalization ability. Thus, better prediction performance has been achieved in comparison with the base classifiers. Reducing the model's bias and the dependence of the predictions on the properties of a training set is important and is reduced by a few coupling models.

In our study, the ensembled model approach was implemented for each person (*one-versus-others*) in distinctive form datasets (one feature set-versus-others' feature sets). These trained machine learning models were fed with complementary sets in terms of the data size that can produce diverse and complying outcomes (own personal/the one or others/the others) [35]. Adversarial-trained LSTM models (LSTM model-1/LSTM model-3) (see Figure 6) are working against each other. And the rest one (BiLSTM model-2) was fed with equal-size features. Finally, the last prediction is conducted by a majority voting

process [36,37]. The testing phase was carried out using feature set-2 on the ensembled RNN models.

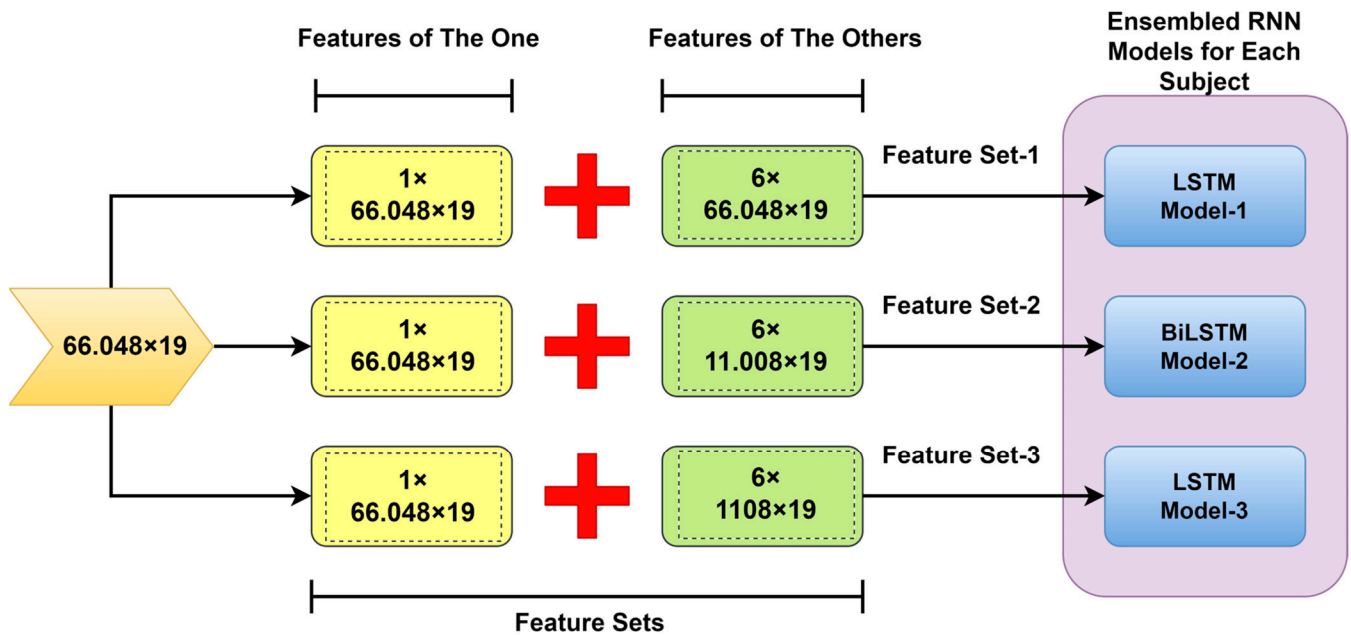


Figure 6. Concatenating the diverse features in the proposed one-versus-others authentication.

Time segments and training size are important critical parameters to provide better biosignal-based biometric systems [38]. The FSST conducted the feature extraction process (see Figure 5). The relevant time segment is defined as 0.5 s over the single-trial EOG sequential time series for the training, testing, and attempts on the ensembled RNN models. Biosignal-based biometrics does not describe the optimal time segment length. Nevertheless, increased time segments are noted that this change only achieves better performances significantly. Furthermore, increased training size can achieve higher biometric system performances, as in the reported works [39]. In our study, an 80–20% rate of data splitting strategy was employed for the training and testing phases, respectively. According to the literature, this rate is the best and optimal rate for providing higher performance for biosignal-biometric systems constructed on RNN deep models [8].

3.5. Fourier Synchrosqueezing Transform (FSST)

The analysis of non-stationary electrophysiological signals requires high-level time-frequency (TF) methods due to the spectral properties of these time-series signals varying over time [30]. Synchrosqueezing transform is an intended advanced TF strategy based on Continuous Wavelet Transform (CWT) and the Short-Time Fourier Transform (STFT) to concentrate sharpens localization of spectral estimation for the oscillation components of a signal. The synchrosqueezing process reassigns “condenses” time-frequency maps around the curves of the instantaneous frequency changes [30]. Hence, FSST is capable of concentrating energy coefficients to obtain compact TF distribution covering TF-based feature extraction vectors. Thus, it may enable high accuracy rates for EOG-based biometric authentication tasks (see Figure 7). STFT determines Fourier transforms while moving along the signal from start to end with a fixed-length window function [30,31]. The related mathematical relations were represented in the following equations. Where R and Re are defined for the round and real part operations, respectively.

$$S(m, k) = \sum_{n=0}^{N-1} x(n)W(n - m)e^{-j\frac{2\pi}{N}k(n-m)} \tag{1}$$

$$\hat{w}[m, k] = \begin{cases} R \left[\operatorname{Re} \left(\frac{N}{2\pi j} \frac{S(m+1, k)}{S(m, k)} \right) \right] & \text{if } S(m, k) \neq 0 \\ 0 & \text{if } S(m, k) = 0 \end{cases} \quad (2)$$

$$FSST(m, \hat{k}) = \sum_{k=0}^{N-1} S(m, k) \delta[\hat{k} - \hat{w}(m, k)] \quad (3)$$

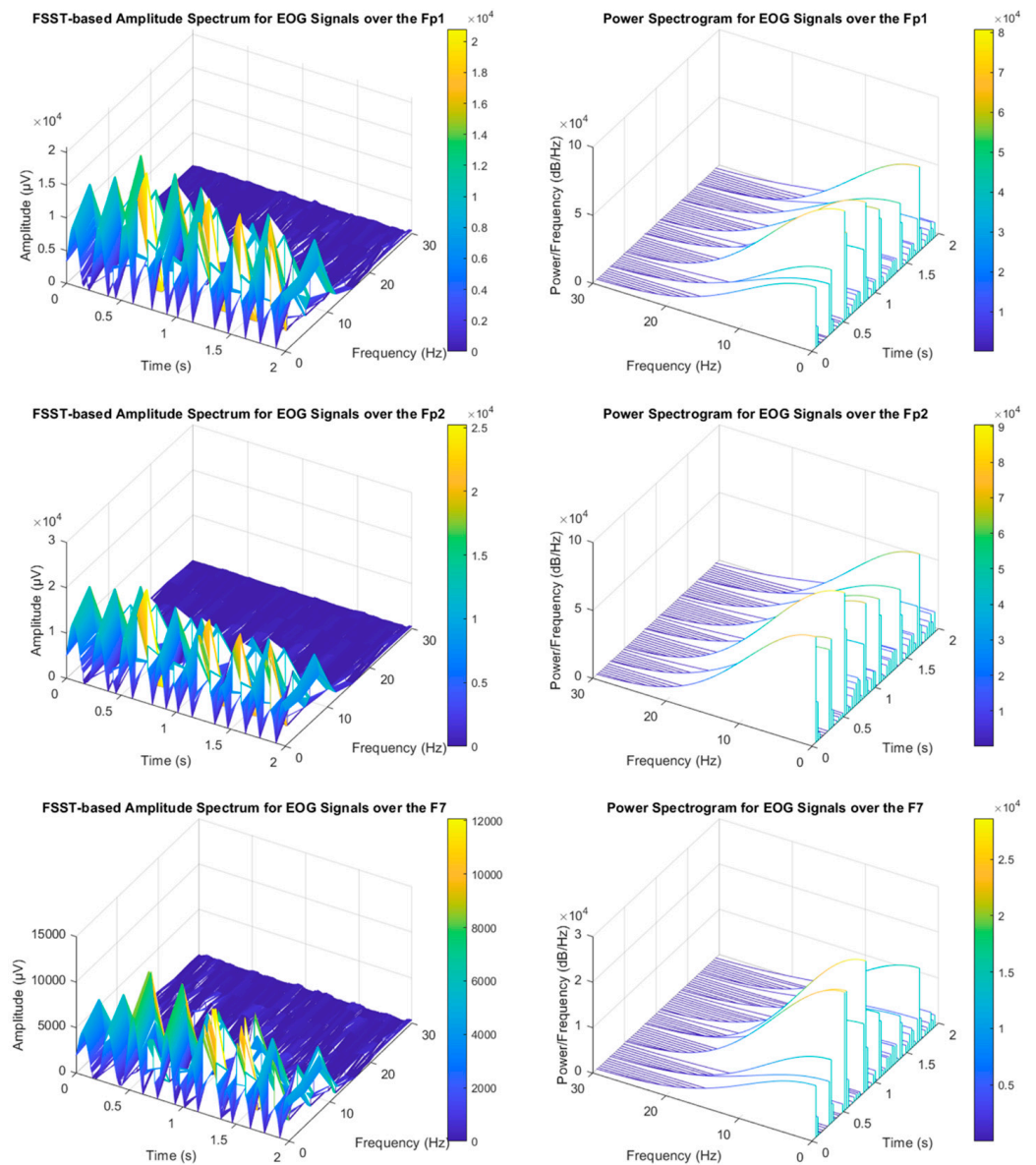


Figure 7. Voluntary eye blinking activities (The relevant EOG signals were collected from the Subject-3).

3.6. Independent Component Analysis (ICA)

Characterizing EOG time-series responses over the multisite EEG recordings is important for developing more reliable and better performance biometric authentication strategies during signal procedures in a framework [40,41]. Multiple electrodes over the scalp are composed of a multiple mixture of independent sources/electrical signals, which occur from the cerebral and/or extracerebral sources [42]. On this point, Independent Component Analysis (ICA) signal processing technique is so effective way to decompose it into a limited number of independent components (ICs) [43]. Here, it defines the multiple channel signals, while the coefficients matrix/mixing matrix and s describe the source

components. Firstly, matrices are calculated with maximum likelihood estimation, and ICs are determined by multiplying the inverse of A by, as seen in the following equations:

$$X = As \tag{4}$$

$$s = A^{-1}X \tag{5}$$

ICA has an important potential application to be considered as a powerful statistical technique for multichannel responses of a unique pattern while decomposing mixed signals into statistical ICs [34].

Recurrence plot (RP) is a recent analysis technique for nonlinear and dynamic activity of biological signals. This method can focus on the repeating patterns of the time-series signals over states and can define geometric structures to visualize the recurrent occurrences of states as a phase space [44]. In this research, RP was employed to visualize the decomposition success over the sequential channels (Fp1–Fp2) for the raw EOG signals and decomposed responses via ICA and EMD (see Figure 8). Long vertical line is able to describe responses, occurred the same state during some time steps [45]. Here, the related segments of this case for signals mean staying in the same phase space region for a short while, and it can be dominated by slow (theta or alpha) waves, including EOGs (8–15 Hz). Thus, high-frequency components can vanish, and slow waves are shown as longer times leading to the up-slope/down-slope patterns [45].

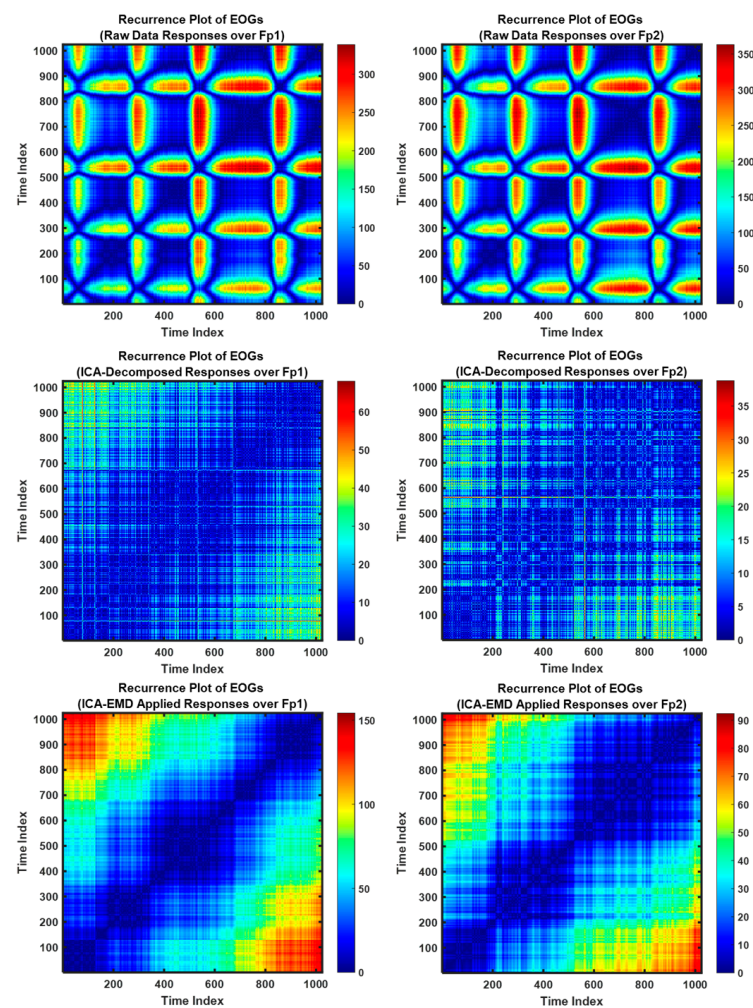


Figure 8. Recurrence plots of EOGs generated via voluntary eye blinkings.

The Figure 8 represents the raw data signals and ICA/EMD applied responses, respectively/top-to-bottom. Moreover, the relevant signals are plotted from the Subject-3 during 1 s and distinct responses are to show the success of ICA/EMD decomposition techniques over the sequential channels.

3.7. Empirical Mode Decomposition (EMD)

The Empirical Mode Decomposition algorithm is considered an adaptive and data-dependent technique to decompose non-linear and non-stationary signals into a set of amplitude-modulated and frequency-modulated components called Intrinsic Mode Functions (IMFs) [14]. This separating analysis way is a powerful time–frequency analysis technique expressing the internal modes’ instantaneous frequency. IMFs include relevant and instant frequency information to obtain frequency values that change over time to offer better time resolution compared to ones. Thus, EMD is to facilitate EOG isolation from EEG signals/ and it is employed voluntary eye blinks extraction from the scalp-recorded EEGs in EOG-based biometric authentication [14,41].

$$x(t) = \sum_{m=0}^k IMF_m(t) + rk(t) \tag{6}$$

In the relevant formula, k defines the IMF number, and $rk(t)$ stands for the final residual value. In this work, the eye blinking waveforms were extracted using EMD according to following last four IMFs and residual value (Isolated EOGs = IMF-2 + IMF-3 + IMF-4 + IMF-5 + Residual) (see Figure 9) [14].

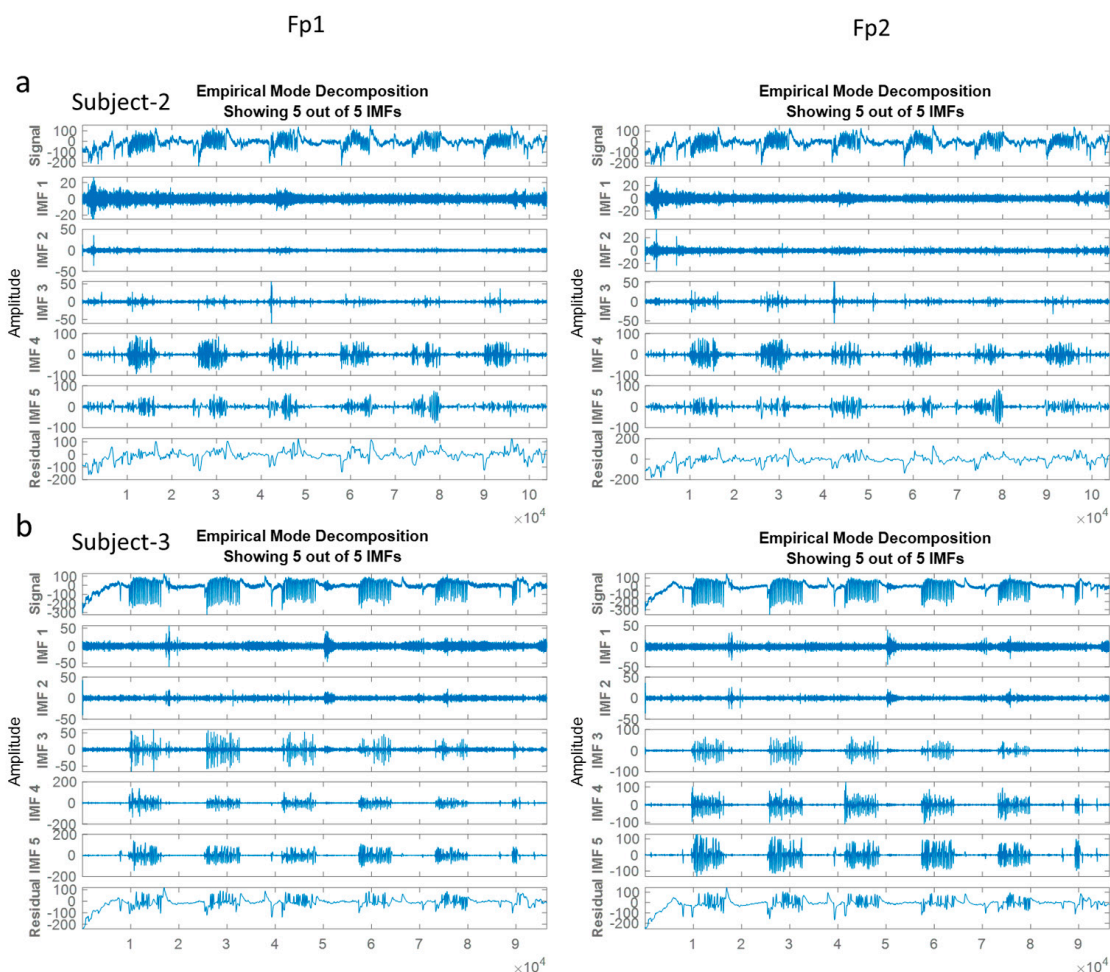


Figure 9. Isolation process of EOG components from the EEGs via EMD.

The plotted signals in Figure 9 are recorded over the Fp1 channel and Fp2 channel in the left and right side, respectively. X-axis is to show the time in seconds and the Y-axis is the amplitude in μV .

3.8. Recurrent Neural Network (RNN) Deep Models

RNN-based deep model networks are able to perceive patterns from the sequential data via the learning of previous experiences when they encounter over time [46]. This ability provides a better recognition level for biological-based time-series signals, including EEGs. The existence of a correlation between the sequential time-series signals stored at different time intervals is named the term ‘long-term dependence’ [47]. Storing and transmitting the state information aims to process the sequences in the RNN deep models. LSTM is designed as a special type of RNN deep model and is capable of observing a correlation between the data learned [48].

On this point, if $x_i \in \mathbb{R}^d$ are defined as a time-series input vector $[x_1, x_2, \dots, x_k]$ and Long-Short Term Memory (LSTM) is able to generate a hidden sequence $[h_1, h_2, \dots, h_k]$ for each processing step [49,50]. The current input function (x_t) and the previous hidden state/feedback into the neuron (h_{t-1}) are both formulating the activation of the hidden state at time t [50]. Hence, this model is different from the CNN (Convolutional Neural Network) deep model [51]. 2D-CNN deep models extract deep features from the images [52] and are evaluated in image processing applications [53]. This related process is as the following term:

$$h_t = f(x_t, h_{t-1}) \quad (7)$$

LSTM deep model has three modules in terms of the different gate combinations. The names of these gates are the forgotten f_t , input i_t and output gates o_t . The transmitted size of information is determined for the next stage in the forgotten gates implementing the sigmoid function in this operation. The next step task is to decide the relevant information to be stored with the sigmoid function at the input gate. Then, the new state information is carried out for the memory cell in the system output [47]. The mathematical formulas are as follows:

$$i_t = \sigma(W_i \cdot [h_{t-1}, x_t] + b_i) \quad (8)$$

$$\tilde{C}_t = \tanh(W_C \cdot [h_{t-1}, x_t] + b_C) \quad (9)$$

$$C_t = f_t * C_{t-1} + i_t * \tilde{C}_t \quad (10)$$

$$o_t = \sigma(W_o \cdot [h_{t-1}, x_t] + b_o) \quad (11)$$

$$h_t = o_t * \tanh(C_t) \quad (12)$$

where, according to the general terms, W is the weight vector, b defines the bias term, σ stands for the sigmoid activation function to put non-linearity. Hence, the new status information of the memory cell is calculated. Moreover, Bidirectional-LSTM (Bi-LSTM) calculates the sequential data in both directions (forward and backward propagation). In the first step, the model performs from the first value of the sequence to the last value. Then, the starting point is performed from the last time value to the first time value (see Figure 10) [47]. The models have been designed with multiple neuron numbers (200) and a fully connected layer (1 neuron). Finally, a softmax classification layer was added to the architecture. The activation function was ReLU, and the optimizer was chosen as Adam. The initial learning rate was defined as 1×10^{-3} . The training process epoch was selected as 300. Table 3 concerns a literature survey summarizing EEG-based authentication and limited EOG-based authentication research in recent years, including RNN-based deep models.

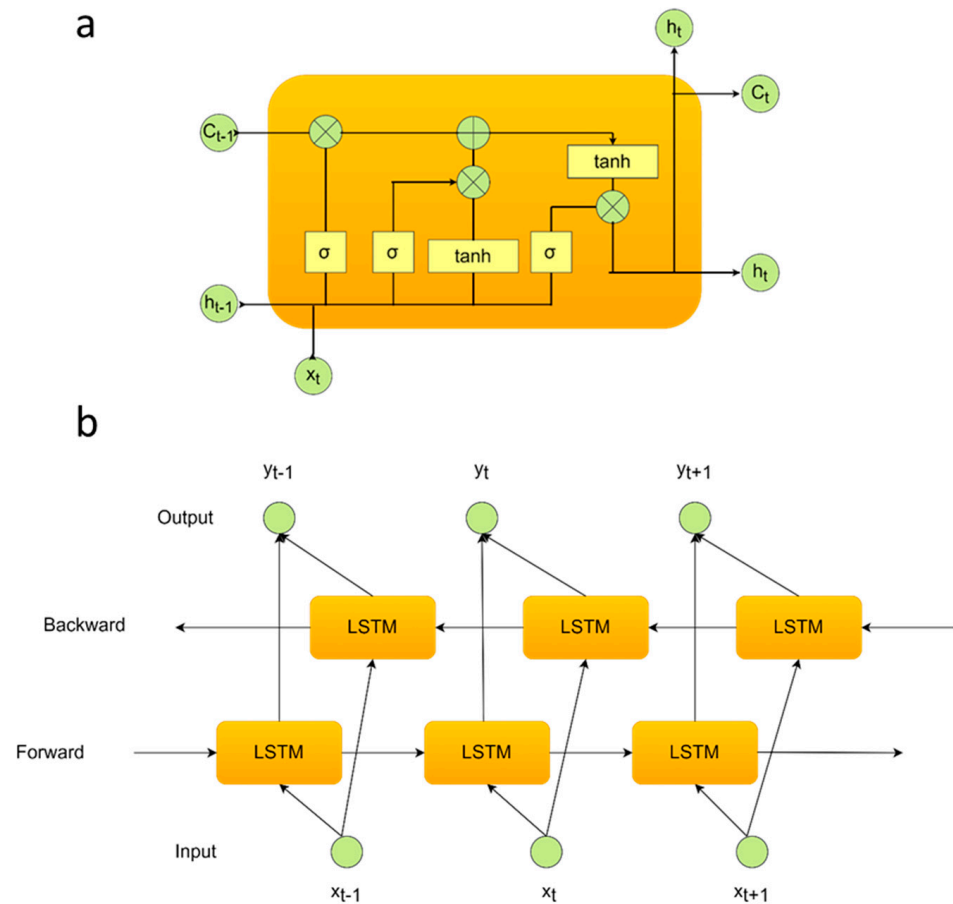


Figure 10. The internal architectures of the (a) LSTM and (b) BiLSTM deep models.

3.9. Performance Metrics

The performance metrics are reported as a key to evaluating machine learning models in pattern recognition tasks and finding the optimal method for solving a problem. The selection of appropriate metrics is critical in data science [48]. A confusion matrix (see Figure 11) is employed to create the other metrics frequently from the fundamental metrics (true positive/TP, true negative/TN, false positive/FP, false negative/FN).

		Predicted	
		Positive	Negative
Actual	Positive	True Positive (TP)	False Negative (FN)
	Negative	False Positive (FP)	True Negative (TN)

Figure 11. The confusion matrix schematic.

Table 3. Concise comparative analysis of EOG and EEG-based biometric authentication performances in recent years.

Ref./Year	Signals	Ch. N.	Sb. N.	S./T.	S. M.	Feature Engineering/Models	Performance
[54]/2019	VEP-EEG	9	25	2	Offline	CCA/Task-Related Component Analysis	ACC: 99.43–100%
[55]/2020	VEP-EEG	32	32	32	Offline	Raw, PSD/CNN-LSTM, CNN-GRU and SVM	ACC: 33.02–100%
[56]/2020	VEP, MI-EEG	19	45	4	Offline	Raw/CNN, CNN-RNN and LDA-SVM	ACC: 77.9–86.9%
[3]/2020	MI-EEG	64	109	10	Offline	EMD, DWT/SVM and Local Outlier Factor (LoF)	TAR: 100% FAR: 0.2%
[57]/2021	VEP-EEG	14	70	10	Offline	DWT/CNN-LSTM	ACC: 81.78–91.93% TAR: 92.86% FAR: 29.28%
[35]/2021	VEP-EEG	9	15	1–10	Online/Offline	Pearson's Correlation Coefficient/Task-Related Component Analysis	ACC: 70.27–100%
[58]/2022	MI-EEG	64	109	14	Offline	Gram-Schmidt Orthogonalization Process/CNN	ACC: >98% TAR: >98% FAR: <2%
[40]/2023	MI-EEG	19	7	1	Offline	FSST, ICA, DWT/Ensembled LSTMs	ACC: ≥ 96.76
[15]/2013	EOG/VOG	≥ 1	19–40	40	Offline	Linear Discriminant Analysis, Quadratic Discriminant Analysis, Naïve Bayesian Rule, k-Nearest Neighbors Support Vector Machine, Discriminant Analysis/EMD/Time Delineation Feature Engineering Gated Recurrent Unit/Time Delineation Feature Engineering	ACC: 53–99%
[14]/2015	EOG	1	25	6–8	Offline	FSST + ICA + EMD/Ensembled RNNs	ACC: $\geq 97\%$ EER: 3.7%
[13]/2020	EOG	14	46	2	Offline	FSST + ICA + EMD/Ensembled RNNs	ACC: 98.7%
Our Study	EOG	19	7	1	Offline	FSST + ICA + EMD/Ensembled RNNs	ACC: $\geq 99\%$ TAR: 99.57% FAR: $\leq 3.33\%$

Ch.N: Channel Number, **Sb.N:** Subject Number, **S.T:** Session/Trial, **S.M:** System Mode, **VEP:** Visual Evoked Potential-EEG, **MI:** Motor Imagery-EEG, **VOG:** Video-Oculography, **EER:** Equal Error Rate.

The number of correct predictions to the total number of predictions yielding the quality metric called classification accuracy (ACC). However, ACC is not accepted as an adequate parameter to determine the proposed algorithm's performance totally. Hence, the other statistical performance metrics are described, including specificity (SPEC), sensitivity (SENS), precision (PREC), and F-score in this respect [48]. The F-score is the coherent coefficient of the precision and sensitivity [59]. The notations are below:

$$ACC = \frac{TP + TN}{TP + TN + FP + FN} \quad (13)$$

$$SPEC = \frac{TN}{TN + FP} \quad (14)$$

$$SENS = \frac{TP}{TP + FN} \quad (15)$$

$$PREC = \frac{TP}{TP + FP} \quad (16)$$

$$F - Score = 2X \frac{PREC \times SENS}{PREC + SENS} \quad (17)$$

Another important metric is the Information Transfer Rate (ITR) to express the amount of information transferred per unit time, especially for Brain-Computer Interfaces area. The mathematical formula is based on the logarithmic:

$$B = \log_2 N + P \log_2 P + (1 - P) \log_2 \frac{(1 - P)}{(N - 1)} \quad (18)$$

where B stands for the number of bits per trial, N is indicating class number, and the correctness of prediction is names as P [47]. The ROC curve is plotted to visualize graph of the false-positive rate (X -axis) and a true-positive rate (Y -axis) and The area under the ROC curve provides the AUC value between the interval $[0, 1]$. The greater AUC value is regarded as better discrimination [47].

In order to calculate the robustness of the biometric authentication systems, the 'True Acceptance Rate' (TAR) and 'False Acceptance Rate' (FAR) are implemented in the developed biometric approaches. Observation of the quality of specific attempts (genuine or forgery) is carried out to take into account verifying a true identity claim (TAR) and the percentage of unauthorized users (FAR) [40]. The expected and successful biometric system is designed to maximize the TAR score while minimizing the FAR score during multiple times of attempts. In this EOG-based biometric approach, 100 attempts were conducted to obtain TAR and FAR scores. Thus, the decision for calculating the TAR and FAR scores was provided after the matching and thresholding process according to the relevant formulas:

$$Decision\ of\ TAR\ (X \setminus Sm) = \begin{cases} Genuine, & \text{if } Sm > th \\ Imposter, & \text{otherwise} \end{cases} \quad (19)$$

$$Decision\ of\ FAR\ (X \setminus Sm) = \begin{cases} Imposter, & \text{if } Sm > th \\ Genuine, & \text{otherwise} \end{cases} \quad (20)$$

where X and th are the query user, and threshold value, respectively. When the similarity matching (Sm) for TAR score is higher than defined th value, the user is treated as genuine else rejected. Otherwise, if the similarity matching (Sm) for FAR score is obtained higher than the defined th , the user is treated as an imposter or else rejected [40]. Threshold levels according to the similarity matching were described as 90% (TAR score) and 80% (FAR score), respectively.

4. Results

This work aims to analyze the performances of seven subjects for the FSST-ICA-EMD framework-based EOG-biometric authentication approach. In order to determine the robustness and outcomes of the *one-versus-others* biometric authentication system, ACC, SENS, SPEC, PREC, F-score, ITR, and AUC scores were determined, as well as finding the TAR and FAR metrics using the ensembled RNN-deep models.

Table 4 highlights the prediction performances of seven participants in the proposed *one-versus-others* EOG-biometric authentication scheme for isolated EOG signals generated by voluntary eye blinkings. According to the results, Subject-7 has achieved high classification performances for all metrics (ACC: 99.99%, SENS: 99.95%, SPEC: 100%, PREC: 99.99%, F-score: 99.95%, AUC: 0.999 and ITR: 0.931) among the others. The worst biometric classification discrimination was calculated on Subject-5 (ACC > 89%, AUC > 0.7, and ITR > 0.9 score). The framework attained the second highest classification performances provided over the Subject-4 (ACC: 99.93% and AUC: 0.997), Subject-1 (ACC: 99.92% and AUC: 0.997), and Subject-3 (ACC: 99.91% and AUC: 0.996), respectively. These biometric prediction results have depicted the number of four individuals reaching up to the >99% (ACC, SENS, SPEC, PREC, and F-score) discrimination regarding the observation metrics.

Moreover, the average of these persons' outcomes has been obtained over >96% accuracy, >0.9 AUC score, and >0.9 ITR value.

Table 4. Biometric approach performances in terms of the discrimination metrics over the EOG signals implemented ICA-EMD techniques.

(%)	Sb1	Sb2	Sb3	Sb4	Sb5	Sb6	Sb7	Avg.
ACC	99.92	92.01	99.91	99.93	89.49	97.00	99.99	96.89
SENS	99.50	64.13	99.42	99.51	57.65	82.88	99.95	86.15
SPEC	100	100	99.99	100	99.92	99.92	100	99.97
PREC	99.92	92.01	99.91	99.93	89.49	97.00	99.99	96.89
F-score	99.50	64.13	99.42	99.51	57.65	82.88	99.95	86.15
AUC	0.997	0.755	0.996	0.997	0.701	0.893	0.999	0.905
ITR	0.971	0.916	0.963	0.936	0.938	0.863	0.931	0.931

Because of the demand for secure user authentication systems, the stable EOG-biometric authentication approach to one specific individual is required under the diverse frequency and speed of eye blinks. In the limited existing literature for EOG-biometric systems, it is reported that spontaneous eye blinkings under a normal physical and emotional state can be influenced by diverse emotions, fatigue, and level of focus as well as the age or light condition. Table 5 defines the proposed system's robustness against its own attempts and imposter attacks in verification mode using two metrics (TAR and FAR). According to the outcomes, the highest scores for TAR were yielded with Subject-3 (100%) and Subject-4 (100%). The other best discrimination (99 attempts out of 100) in the *one-versus-others* biometric authentication for the own attempts are observed in Subject-2, Subject-5, and Subject-6. According to the multiple time sequences of voluntary eye blinks and discrimination performances, Subject-1 and Subject-7 have achieved the least TAR scores at 98% and 96%, respectively. Furthermore, the following FAR metric scores show that Subject-1, Subject-4, and Subject-7 have 0 average values out of 100 attacks for each isolated EOG-based authentication system. The other subjects' own systems have 3.33% (Subject-2 and Subject-5), 1.83% (Subject-3), and 0.5% (Subject-6) in terms of the FAR scores.

Table 5. Biometric approach performances in terms of the matching scores/attempts over the EOG signals implemented ICA-EMD techniques.

(%) *	TAR	FAR							Avg.
		Sb1	Sb2	Sb3	Sb4	Sb5	Sb6	Sb7	
Sb1	98	X	0	0	0	0	0	0	0
Sb2	99	0	X	1	0	19	0	0	3.33
Sb3	100	0	9	X	0	0	2	0	1.83
Sb4	100	0	0	0	X	0	0	0	0
Sb5	99	0	20	0	0	X	0	0	3.33
Sb6	99	0	0	0	3	0	X	0	0.5
Sb7	96	0	0	0	0	0	0	X	0
Avg.	98.71								

* 100 attempts.

The most important technique for EOG + EEG signal decomposition for multiple channels is Independent Component Analysis (ICA). Table 6 presents the prediction results of the EOG-based biometric authentication with EEGs implemented ICA for multiple channel recordings. By analyzing the decomposed multiple channels for EOG + EEG responses in the *one-versus-others* authentication, it defines that all individuals have achieved >99% discrimination accuracies for each authentication case. Totally, the average accuracy, sensitivity, specificity, precision, and F-score prediction outcomes are also higher than 99% value. AUC and ITR scores are also greater than 0.99 values. However, the best

discrimination is observed in Subject-4 in terms of all performance metrics (ACC: 99.93% and AUC: 0.997) during vertical voluntary eye blinkings.

Table 6. Biometric approach performances in terms of the discrimination metrics over the EOG + EEG signals implemented ICA technique.

(%)	Sb1	Sb2	Sb3	Sb4	Sb5	Sb6	Sb7	Avg.
ACC	99.93	99.88	99.93	99.93	99.92	99.91	99.94	99.92
SENS	99.53	99.91	99.79	99.54	99.58	99.54	1	99.70
SPEC	1	99.87	99.95	99.99	99.98	99.97	99.93	99.96
PREC	99.93	99.88	99.93	99.93	99.92	99.91	99.94	99.92
F-score	99.53	99.91	99.79	99.54	99.58	99.54	1	99.70
AUC	0.997	0.998	0.998	0.997	0.997	0.997	0.999	0.998
ITR	0.999	0.992	0.999	0.978	0.993	0.999	0.999	0.994

For the proposed high-level feature engineering with FSST in the EOG-biometric authentication approach, the calculation of the matching score was revealed in Table 7. According to the TAR and FAR scores, the attempts and attacks for the own individual biometric authentication system, including ensembled RNN models, have shown high TAR scores (>99.57%) and low FAR scores (0%) on average. The least matching score for TAR score was obtained in Subject-6 (97%), and the others have provided 100% authentication success out of 100 attempts.

Table 7. Biometric approach performances in terms of the matching scores/attempts over the EOG + EEG signals implemented ICA technique.

(%) *	TAR	FAR							Avg.
		Sb1	Sb2	Sb3	Sb4	Sb5	Sb6	Sb7	
Sb1	100	X	0	0	0	0	0	0	0
Sb2	100	0	X	0	0	0	0	0	0
Sb3	100	0	0	X	0	0	0	0	0
Sb4	100	0	0	0	X	0	0	0	0
Sb5	100	0	0	0	0	X	0	0	0
Sb6	97	0	0	0	0	0	X	0	0
Sb7	100	0	0	0	0	0	0	X	0
Avg.	99.57								

* 100 attempts.

Following the steps above, the behavioral biometric feature of EOG signals recorded over the EEGs was revealed to recognize bioelectrical signal patterns during voluntary eye blinks for person authentication. The following tests compare EOG and EOG-EEG signals in authentication achievement consisting of the discrimination metrics and matching scores (see Figure 12 and Figure 13). Hence, it is clear to be in the observation that EOG-EEG signals have relatively better authentication success, especially in TAR (0.86% higher) and FAR (3.33% lower) similarity scores due to the multi-modality responses. Uniqueness and the biometric characteristics of each subject may be defined better by these two physiological traits.

The t-distributed stochastic neighbor embedding (t-SNE) was employed to specify the discrimination of each individual on the scattering benchmark for comparison [40,60]. A unique colored cluster represented each subject. It also confirmed that the seven individuals had great separable outcomes based on voluntary eye blinkings. Each subject is represented by a unique colored cluster [61,62]. It was clearly observed that there are high intraclass similarity and low interclass similarity with minimal overlap for diverse subjects in the ICA-based dataset, ICA-EMD-based dataset, and FSST-ICA-EMD-based datasets (see Figure 14).

In addition to seven-person separation via t-SNE, the discriminative ability of the *one-versus-others* biometric features were represented in Figure 15.

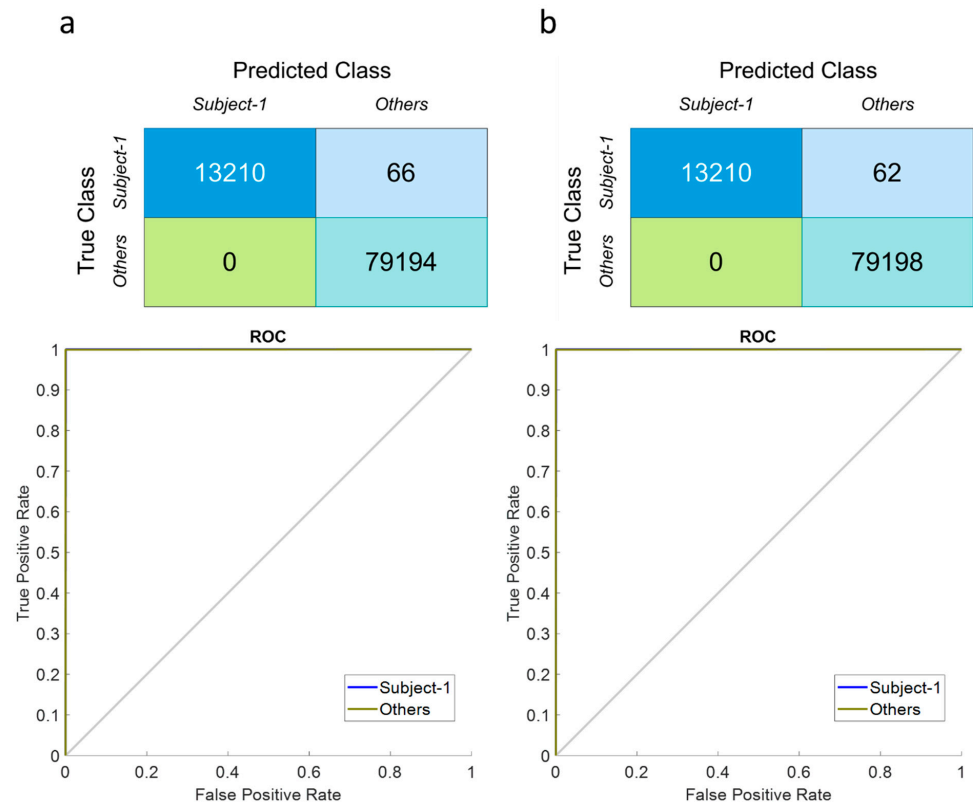


Figure 12. Confusion matrices and ROC curves for EOG-based authentication approach generated via voluntary eye blinks (a) Isolated EOG responses (b) Raw EOG responses with EEGs.

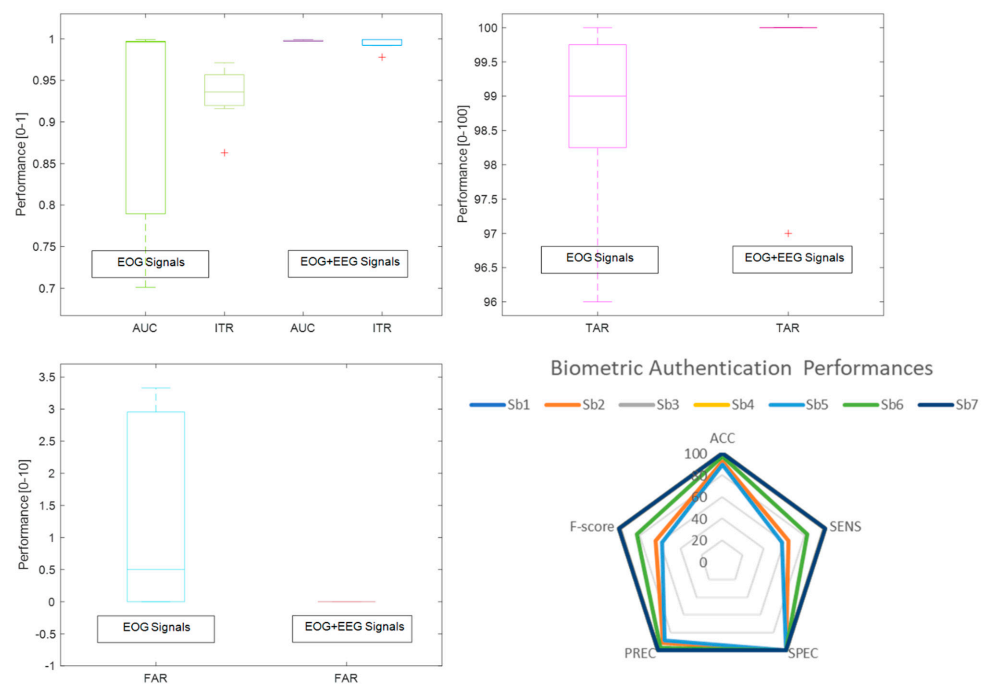


Figure 13. Variations of biometric authentication of AUC/ITR outcomes and TAR/FAR similarity scores for isolated EOG responses and raw EOGs with EEGs (*Whisker box plot*), Discrimination metrics for isolated EOG responses (*Spider plot*).

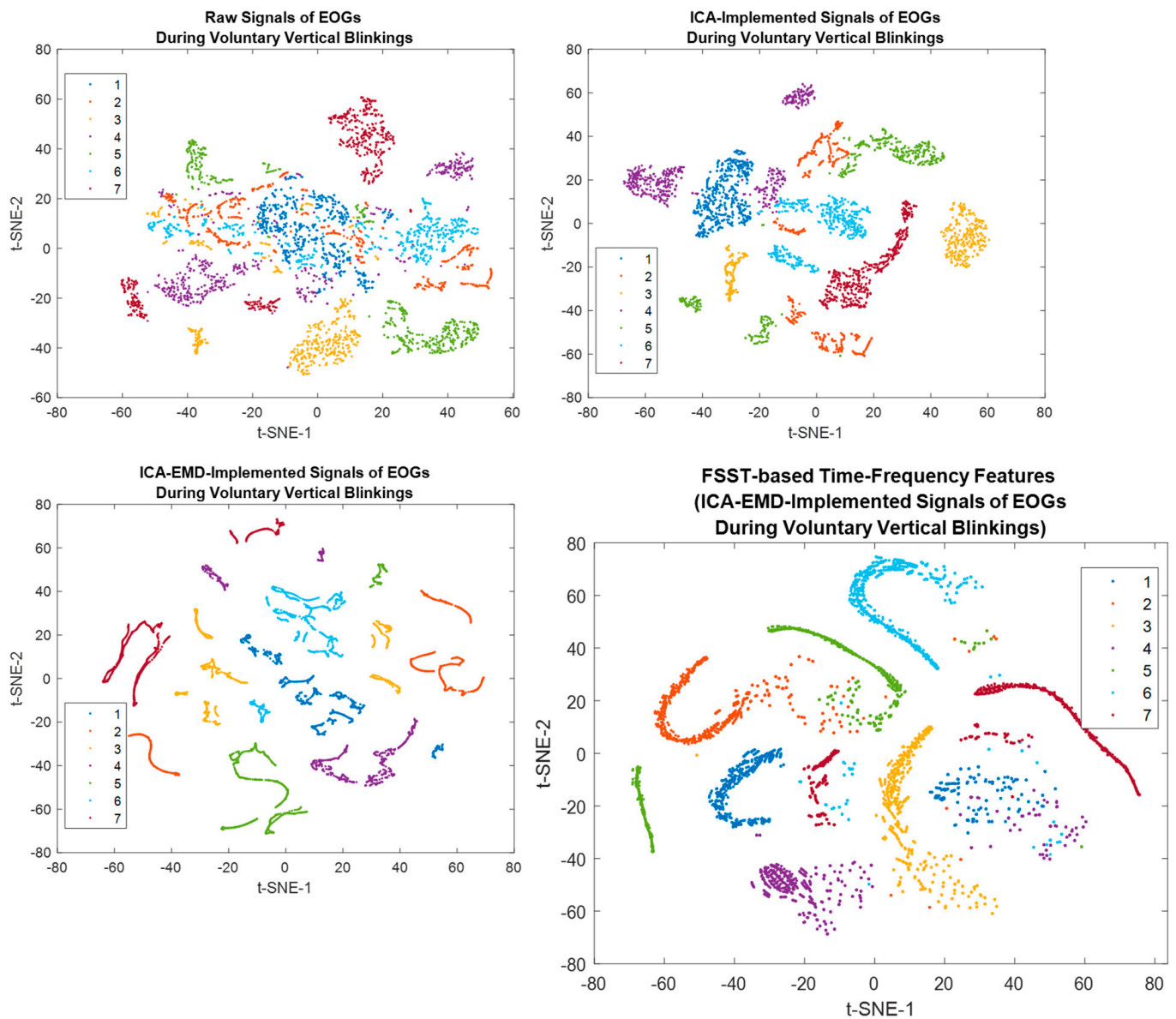


Figure 14. t-distributed stochastic neighbor embedding (t-SNE) plots visualize the separability of the different features (Each colored clusters describe different individuals).

The probability distribution functions (PDFs) of the correlation coefficients between the frontal-lobe electrode locations (Fp1–Fp2 and Fp1–F3) aim to indicate the ability to discriminate among paired subjects. The largest differentiation (the smallest overlap area) means better authentication discrimination, and the smallest differentiation (the largest overlap area) has poor discrimination performances [40]. According to the PDFs, the lowest discrimination among the cross-subjects and same-subjects was obtained between Subject-1 and Subject-2. The highest separability performances were provided with Subject-6 and Subject-7 (see Figure 16). Correlation coefficient matrices might offer to provide a unique pattern for each subject and the relationship between affective discriminability-related cerebral cortex (see Figure 17). These results demonstrate the feasibility and potential robustness of this framework against to intra-session and inter-session variability. Furthermore, the least electrode pairs of related cortices may lead to unique information for each person and the usability of this FSST-ICA-EMD framework-based EOG-biometric authentication approach [40].

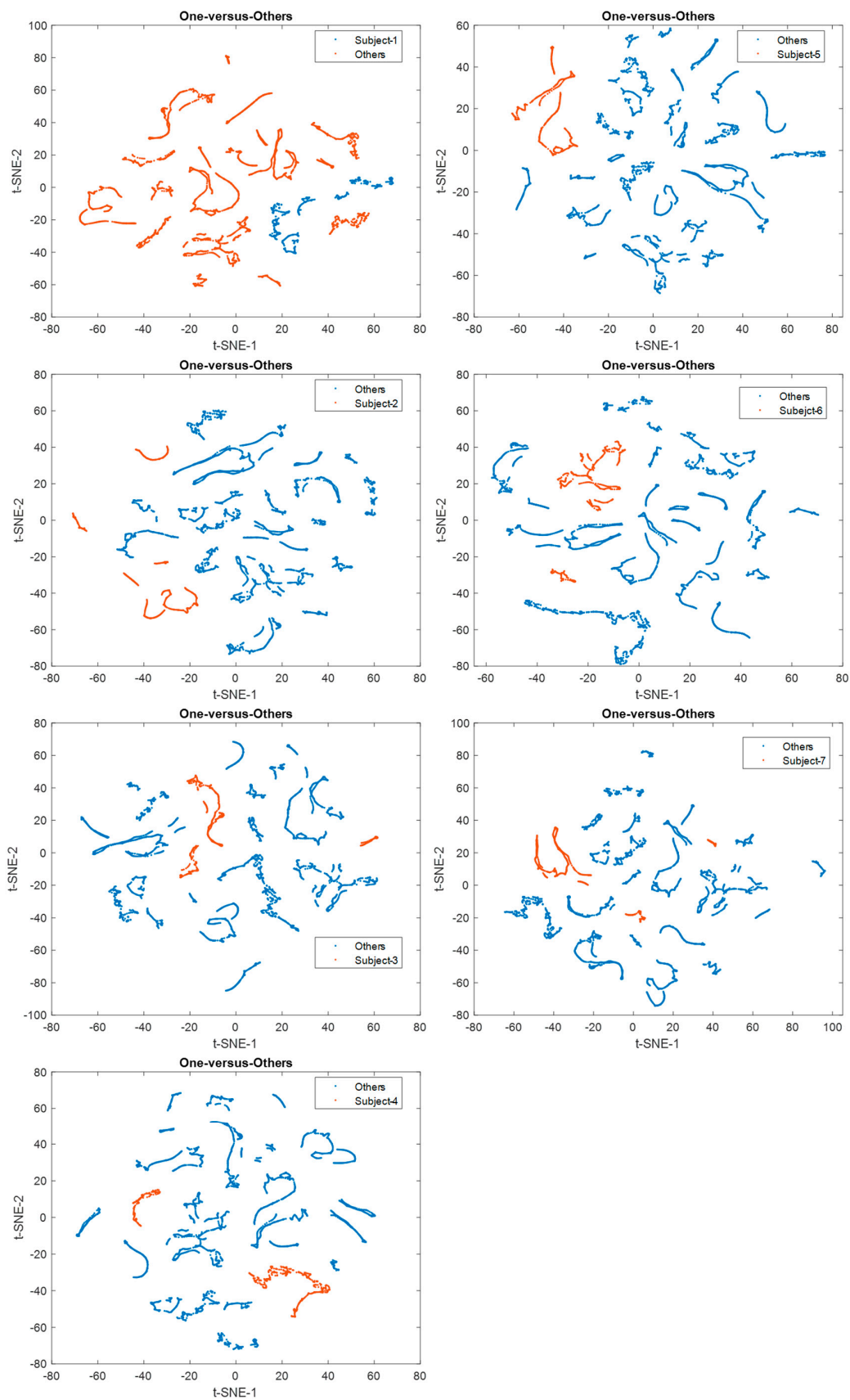


Figure 15. t-SNE plots for the one-versus-others discrimination (ICA-EMD-based datasets were processed for these presentations).

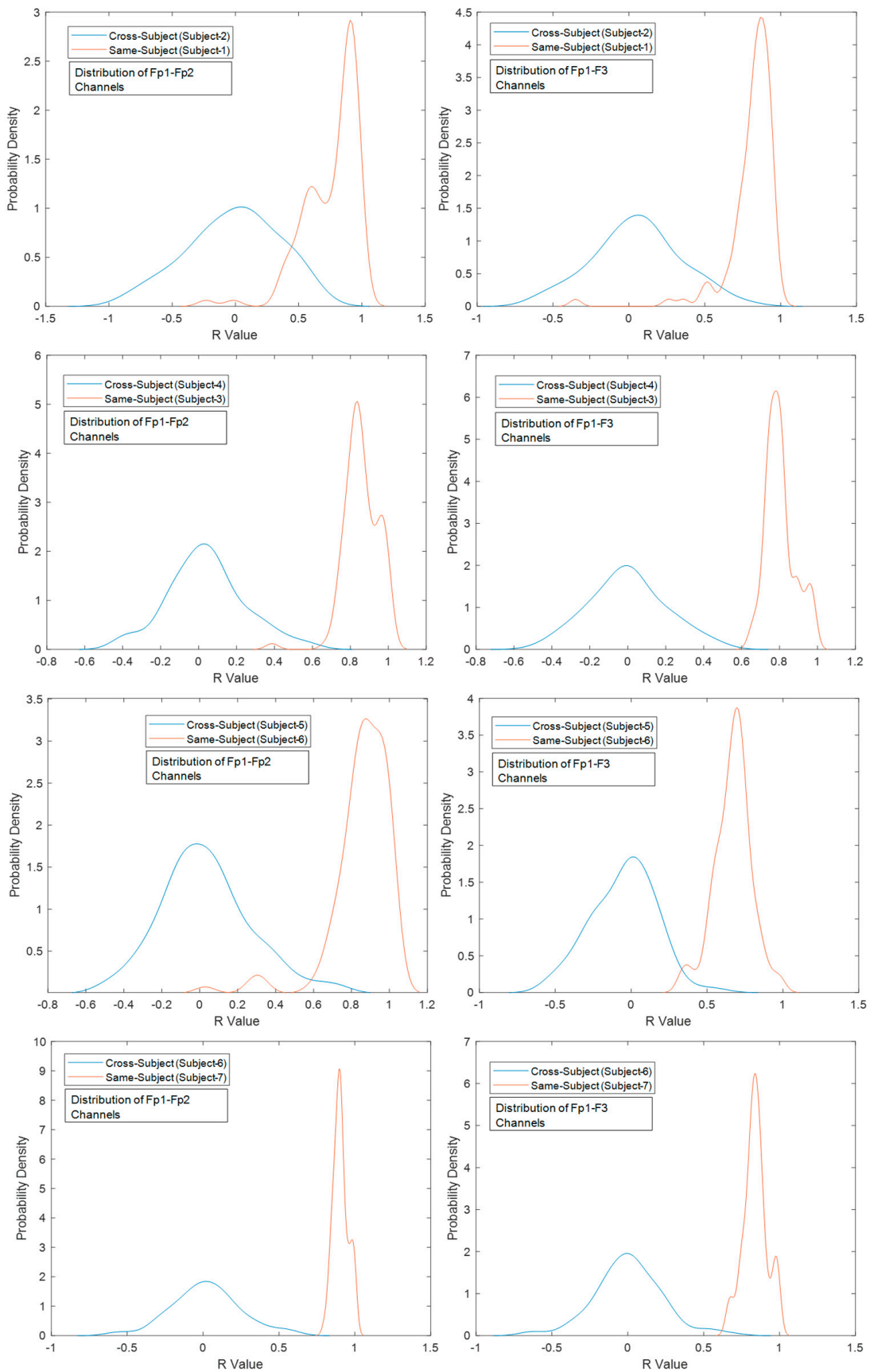


Figure 16. Probability density functions of the correlation coefficients (R value) between the frontal-lobe electrodes under cross-subject and same-subject conditions.

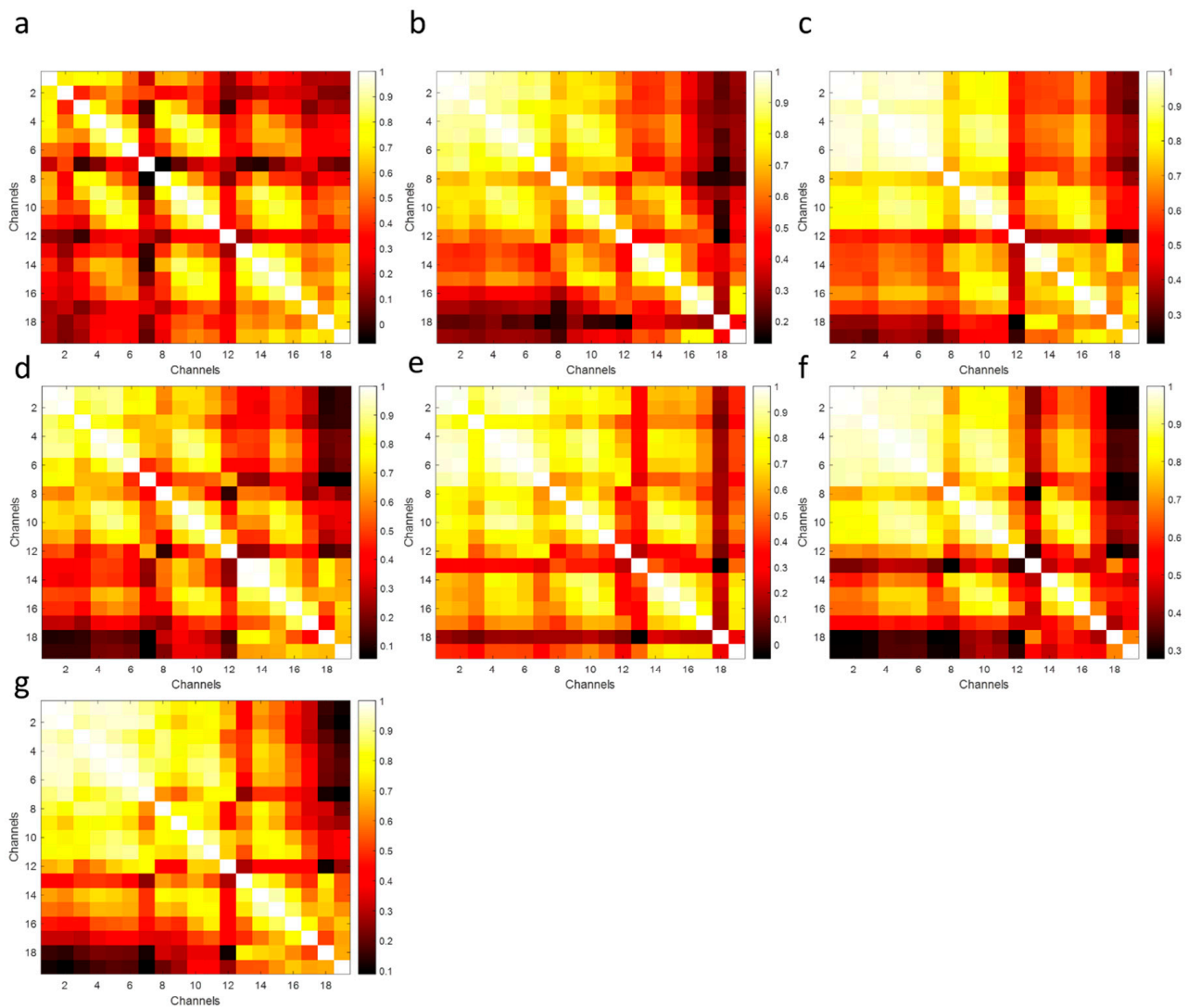


Figure 17. Unique patterns of correlation matrices for each subject related to the electrode locations ((a–g) plots correspond to the Subject-1 to Subject-7, respectively).

Multivariate analysis of variance (MANOVA/ multivariate extension of ANOVA) was implemented to compute group significance and to distribute each person among various FSST time-frequency feature groups [63]. The discrimination ability of the FSST-based framework helps to distinguish each individual by these features. Clustering subjects via MANOVA shows the high group significance separation over the defined scores for each group (Figure 18) [39]. Hence, p -values were determined as less than or equal to 0.05, and these values offer to represent a significant difference among the individuals in terms of the feature-extracted EOGs generated by voluntary eye blinks. The distinctive ability of the features/framework is to maximize for each person, and the MANOVA scores were considered statistically relevant for further analysis in this *one-versus-others* EOG-based biometric authentication. The length of the EOG segments for training/testing phases in the ensembled RNN-based deep models might be investigated to provide less amount of data during enrollment and authentication progress. Thus, a biometric system can be user-friendly due to the minimized evaluation time. MANOVA can be employed to observe the influence of the performance of the EOG-biometric system over the significant scores in different segment lengths [8,39].

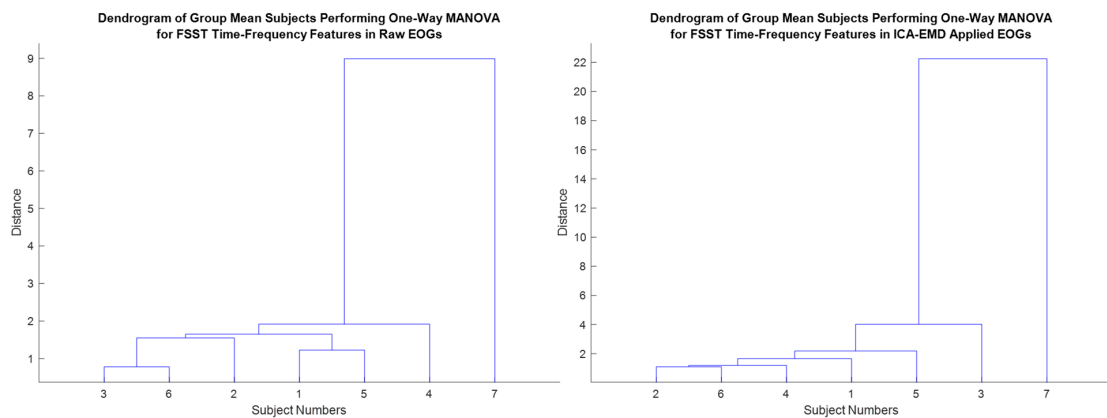


Figure 18. Clustering subjects via MANOVA.

The time-series EOGs responses occur in frequency falling in the range of 0.5–15 Hz/20 Hz and have dynamic and nonstatic characteristics acquired by the origin of the voluntary eye blinkings [14,64]. The channel positions on the scalp were estimated to explore the performances of the raw EOG signals in the FSST-ICA-EMD framework-based biometric authentication. A minimal subset of recorded channels is targeted for low computational cost and portability of the equipment in biometric systems [3,40]. These responses correspond to the seven subjects and represent the brain mappings of the unique pattern for each person. The power spectral density outcomes for 15 Hz were plotted to address the temporal-spatial patterns. According to these mappings (see Figure 19 [65]) and functional connectivity (see Figure 20), frontal (high level) and posterior parietal (low level) cortices reveal the action-specific sites during eye blinking activations.

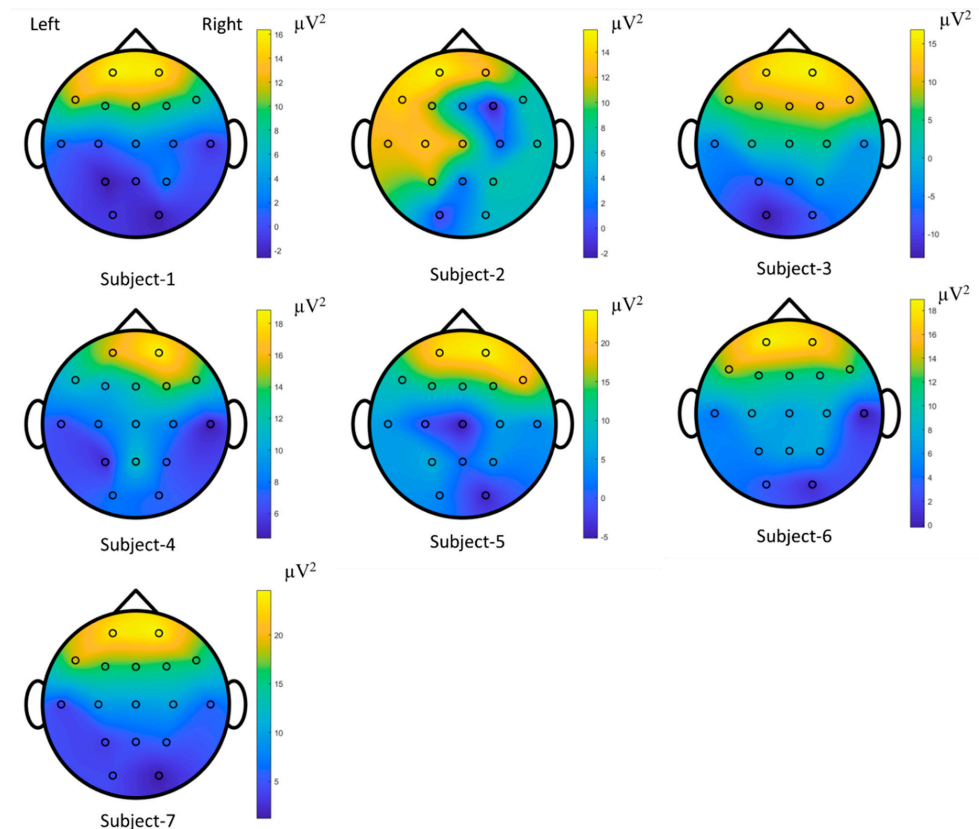


Figure 19. Brain mappings for each individual during the voluntary eye blinkings in EOG-biometric authentication.

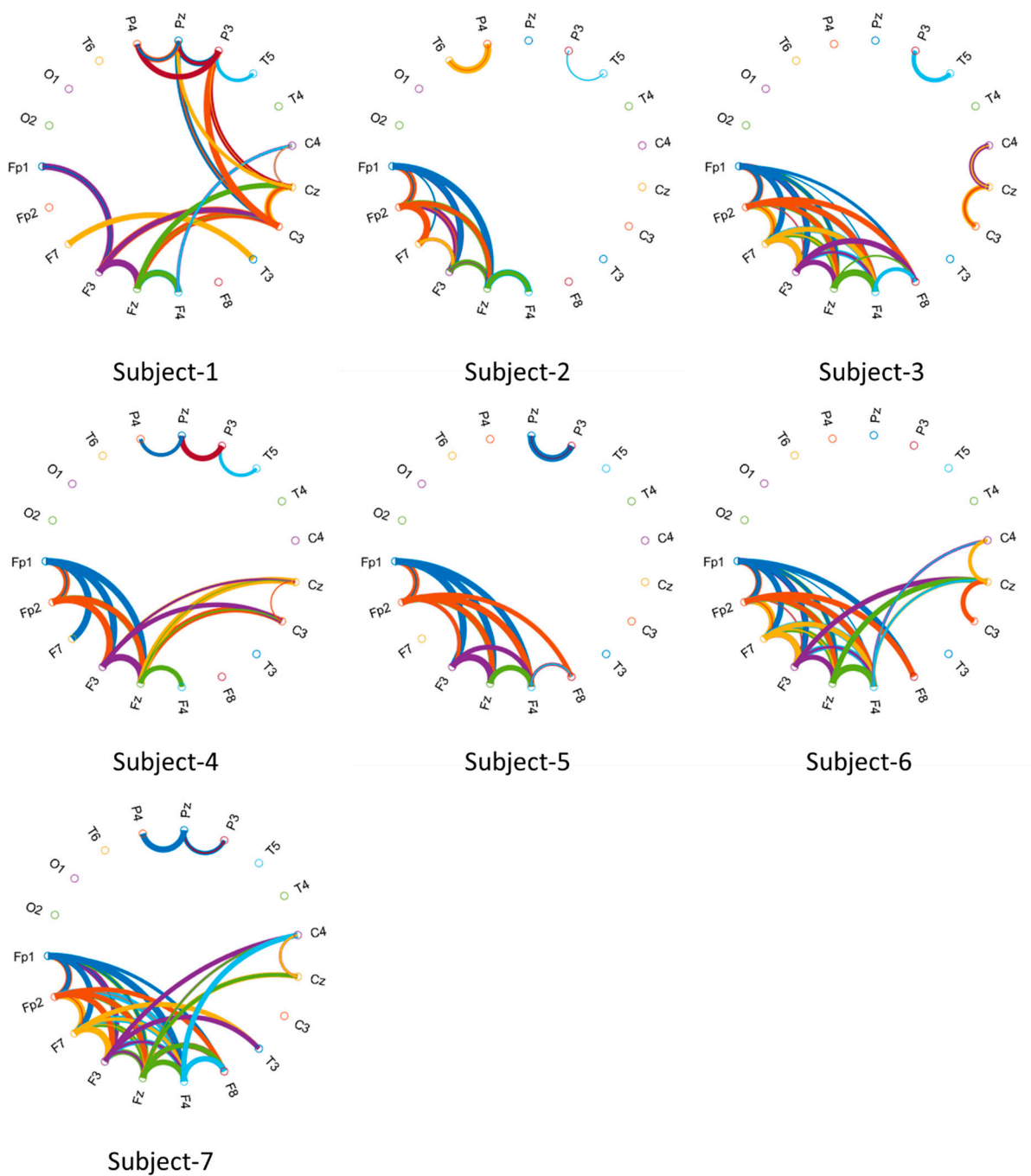


Figure 20. The Circular Graph visualizes the brain’s functional connectivity during the voluntary eye blinkings (Threshold values were applied to draw a clear understanding of functional connectivity over the correlation matrix for each subject).

Furthermore, Circular Graphs (CGs) were described to calculate the correlation of scalp locations introducing the dynamics of functional connectivity across multiple channels [66,67]. Visualization functionality during voluntary eye blinkings for the biometric systems is important to observe nonlinear connectivity in every EOG recording. The connectivity values between channels were handled to draw the lines connecting the two channels. The drawn width on the circumference of the circle is to represent the correlation strength of the connection [68]. The lines were highly connected, clearly marking the frontal-to-other cortices in both hemispheres.

The major drawback for EEG-biometric systems is the instability issue over time due to the environment and mental state fatigue [40]. However, voluntarily generated EOG responses are much more stable than EEGs, leading to more reliable authentication progress. The other primary advantage of this FSST-ICA-EMD framework-based EOG-biometric authentication is to offer fast enrollment and authentication time with high TAR ($\geq 98\%$) and low FAR ($\leq 3.33\%$) scores via processing low time-segment (0.5 s). In the limited existing biosignal-related biometric research, few of them concern low-time segment conditions [40,56].

5. Conclusions

To address some of the aforementioned issues, we have developed robust (high TAR scores: $\geq 98\%$ and low FAR scores: $\leq 3.33\%$) and high verification accuracy (ACC: 99.99% and AUC: 0.99) FSST-ICA-EMD framework-based EOG-biometric authentication approach using ensembled RNN-deep models during voluntary eye blinking activities. Our objective was to form as voluntary straightforward verification task as possible since this robust framework-based EOG-biometric approach has enabled a 0.5-s short measurement (time-segment) in training/testing/attempts of a single trial. Thus, it may be capable of high access enrollment/authentication phases in real-time usage in future research. With the COVID-19 pandemic and quarantines, the education system has been abruptly transformed into distance and online courses under e-learning applications [17,18]. Hence, FSST-ICA-EMD framework-based EOG-biometric authentication to this e-learning platform may offer sustainable, continuous, effective strategies and procedures.

Future Work

Different adaptations and experiments have been left for future work due to a lack of time. Firstly, the limitation of this work has multiple electrode usage. However, this challenge can be updated in future works by considering the functional connectivity plots and brain mappings for limited and effective channels with dry and Bluetooth electrode technologies. In this biometric system, RNN-based ensembled models were implemented for better-recognizing time-series EOG signals. Moreover, leveraging transfer learning can be applied to state-of-the-art deep learning models and other biosignals/images to provide multimode biometric strategies [69,70]. Also, pre-trained networks and fuzzy-based expert system can be investigated on this EOG-biometric system [71,72]. Furthermore, real-time authentication experiments can be done on the students while accessing the e-learning platforms.

Funding: This research received no external funding.

Institutional Review Board Statement: The study was conducted in accordance with the Declaration of Helsinki, and approved by the Institutional Review Board (or Ethics Committee) of Bandirma Onyedi Eylul University (protocol code 2020-26 and date of approval) for studies involving humans.

Data Availability Statement: The materials used in this research as high-quality EEG files of volunteers can be sent upon the request.

Acknowledgments: This study was supported by the Scientific Research Project Unit of the Bandirma Onyedi Eylul University under the project no; BAP-20-1004-002.

Conflicts of Interest: The authors declare no conflict of interest.

Human and Animal Rights: The study was approved by the Ethical Committee of Bandirma Onyedi Eylul University under document number 2020-26. Informed consent was obtained from all subjects involved in the study. Written informed consent has been obtained from the patient(s) to publish this paper.

References

1. Dargan, S.; Kumar, M. A Comprehensive Survey on the Biometric Recognition Systems Based on Physiological and Behavioral Modalities. *Expert Syst. Appl.* **2020**, *143*, 113114. [[CrossRef](#)]
2. Behera, S.K.; Kumar, P.; Dogra, D.P.; Roy, P.P. A Robust Biometric Authentication System for Handheld Electronic Devices by Intelligently Combining 3D Finger Motions and Cerebral Responses. *IEEE Trans. Consum. Electron.* **2021**, *67*, 58–67. [[CrossRef](#)]
3. Moctezuma, L.A.; Molinas, M. Towards a Minimal EEG Channel Array for a Biometric System Using Resting-State and a Genetic Algorithm for Channel Selection. *Sci. Rep.* **2020**, *10*, 14917. [[CrossRef](#)] [[PubMed](#)]
4. Jayarathne, I.; Cohen, M.; Amarakeerthi, S. Person Identification from EEG Using Various Machine Learning Techniques with Inter-Hemispheric Amplitude Ratio. *PLoS ONE* **2020**, *15*, e0238872. [[CrossRef](#)]
5. Tatar, A.B. Biometric Identification System Using EEG Signals. *Neural Comput. Appl.* **2023**, *35*, 1009–1023. [[CrossRef](#)]
6. Chen, Y.; Atnafu, A.D.; Schlattner, I.; Weldtsadik, W.T.; Roh, M.-C.; Kim, H.J.; Lee, S.-W.; Blankertz, B.; Fazli, S. A High-Security EEG-Based Login System with RSVP Stimuli and Dry Electrodes. *IEEE Trans. Inf. Forensics Secur.* **2016**, *11*, 2635–2647. [[CrossRef](#)]
7. Moctezuma, L.A.; Molinas, M. Multi-Objective Optimization for EEG Channel Selection and Accurate Intruder Detection in an EEG-Based Subject Identification System. *Sci. Rep.* **2020**, *10*, 5850. [[CrossRef](#)]
8. Jyotishi, D.; Dandapat, S. An LSTM-Based Model for Person Identification Using ECG Signal. *IEEE Sensors Lett.* **2020**, *4*, 1–4. [[CrossRef](#)]
9. Ortega-Rodríguez, J.; Gómez-González, J.F.; Pereda, E. Selection of the Minimum Number of EEG Sensors to Guarantee Biometric Identification of Individuals. *Sensors* **2023**, *23*, 4239. [[CrossRef](#)]
10. Biswas, D.; Everson, L.; Liu, M.; Panwar, M.; Verhoef, B.-E.; Patki, S.; Kim, C.H.; Acharyya, A.; Van Hoof, C.; Konijnenburg, M.; et al. CorNET: Deep Learning Framework for PPG-Based Heart Rate Estimation and Biometric Identification in Ambulant Environment. *IEEE Trans. Biomed. Circuits Syst.* **2019**, *13*, 282–291. [[CrossRef](#)]
11. Gorur, K.; Bozkurt, M.R.; Bascil, M.S.; Temurtas, F. Glossokinetic Potential Based Tongue–Machine Interface for 1-D Extraction Using Neural Networks. *Biocybern. Biomed. Eng.* **2018**, *38*, 745–759. [[CrossRef](#)]
12. Abo-Zahhad, M.; Ahmed, S.M.; Abbas, S.N. A New Multi-Level Approach to EEG Based Human Authentication Using Eye Blinking. *Pattern Recognit. Lett.* **2016**, *82*, 216–225. [[CrossRef](#)]
13. Jalilifard, A.; Chen, D.; Mutasim, A.K.; Bashar, M.R.; Tipu, R.S.; Shawon, A.-U.K.; Sakib, N.; Amin, M.A.; Islam, M.K. Use of Spontaneous Blinking for Application in Human Authentication. *Eng. Sci. Technol. Int. J.* **2020**, *23*, 903–910. [[CrossRef](#)]
14. Abo-Zahhad, M.; Ahmed, S.M.; Abbas, S.N. A Novel Biometric Approach for Human Identification and Verification Using Eye Blinking Signal. *IEEE Signal Process. Lett.* **2015**, *22*, 876–880. [[CrossRef](#)]
15. Juhola, M.; Zhang, Y.; Rasku, J. Biometric Verification of a Subject through Eye Movements. *Comput. Biol. Med.* **2013**, *43*, 42–50. [[CrossRef](#)] [[PubMed](#)]
16. Chen, G.; Wang, F.; Yuan, X.; Li, Z.; Liang, Z.; Knoll, A. NeuroBiometric: An Eye Blink Based Biometric Authentication System Using an Event-Based Neuromorphic Vision Sensor. *IEEE/CAA J. Autom. Sin.* **2021**, *8*, 206–218. [[CrossRef](#)]
17. Labayen, M.; Vea, R.; Florez, J.; Aginako, N.; Sierra, B. Online Student Authentication and Proctoring System Based on Multimodal Biometrics Technology. *IEEE Access* **2021**, *9*, 72398–72411. [[CrossRef](#)]
18. Gurcan, F.; Dalveren, G.G.M.; Derawi, M. COVID-19 and E-Learning: An Exploratory Analysis of Research Topics and Interests in E-Learning during the Pandemic. *IEEE Access* **2022**, *10*, 123349–123357. [[CrossRef](#)]
19. Gurcan, F.; Boztas, G.D.; Dalveren, G.G.M.; Derawi, M. Digital Transformation Strategies, Practices, and Trends: A Large-Scale Retrospective Study Based on Machine Learning. *Sustainability* **2023**, *15*, 7496. [[CrossRef](#)]
20. Ubah, A.E.; Onakpojeruo, E.P.; Ajamu, J.; Mangai, T.R.; Isa, A.M.; Ayansina, N.B.; Al-Turjman, F. Biometrics Authentication Techniques in E-Learning Assessment. In Proceedings of the 2022 International Conference on Artificial Intelligence of Things and Crowdsensing (AIoTCs), Nicosia, Cyprus, 26–28 October 2022; pp. 126–132.
21. Acien, A.; Morales, A.; Monaco, J.V.; Vera-Rodriguez, R.; Fierrez, J. TypeNet: Deep Learning Keystroke Biometrics. *IEEE Trans. Biom. Behav. Identity Sci.* **2022**, *4*, 57–70. [[CrossRef](#)]
22. Haque, M.A.; Haque, S.; Zeba, S.; Kumar, K.; Ahmad, S.; Rahman, M.; Marisennayya, S.; Ahmed, L. Sustainable and Efficient E-Learning Internet of Things System through Blockchain Technology. *E-Learn. Digit. Media* **2023**, 204275302311567. [[CrossRef](#)]
23. Chahal, J.; Rani, N. Exploring the Acceptance for E-Learning among Higher Education Students in India: Combining Technology Acceptance Model with External Variables. *J. Comput. High. Educ.* **2022**, *34*, 844–867. [[CrossRef](#)] [[PubMed](#)]
24. Fenu, G.; Marras, M.; Boratto, L. A Multi-Biometric System for Continuous Student Authentication in e-Learning Platforms. *Pattern Recognit. Lett.* **2018**, *113*, 83–92. [[CrossRef](#)]
25. Kumar, K.; Al-Besher, A. IoT Enabled E-Learning System for Higher Education. *Meas. Sens.* **2022**, *24*, 100480. [[CrossRef](#)]
26. Aslam, S.M.; Jilani, A.K.; Sultana, J.; Almutairi, L. Feature Evaluation of Emerging E-Learning Systems Using Machine Learning: An Extensive Survey. *IEEE Access* **2021**, *9*, 69573–69587. [[CrossRef](#)]
27. Rukhiran, M.; Wong-In, S.; Netinant, P. User Acceptance Factors Related to Biometric Recognition Technologies of Examination Attendance in Higher Education: TAM Model. *Sustainability* **2023**, *15*, 3092. [[CrossRef](#)]
28. Sun, Y.; Nembhard, D.A. Static vs. Dynamic Representations and the Mediating Role of Behavioral Affect on E-Learning Outcomes. *Int. J. Hum. Comput. Interact.* **2022**, 1–12. [[CrossRef](#)]

29. Bogicevic Sretenovic, M.; Milenkovic, I.; Jovanovic, B.; Simic, D.; Minovic, M.; Milovanovic, M. Bringing Biometric Sensors to the Classroom: A Fingerprint Acquisition Laboratory for Improving Student Motivation and Commitment. *Appl. Sci.* **2020**, *10*, 880. [CrossRef]
30. Madhavan, S.; Tripathy, R.K.; Pachori, R.B. Time-Frequency Domain Deep Convolutional Neural Network for the Classification of Focal and Non-Focal EEG Signals. *IEEE Sens. J.* **2020**, *20*, 3078–3086. [CrossRef]
31. Ozel, P.; Akan, A.; Yilmaz, B. Synchrosqueezing Transform Based Feature Extraction from EEG Signals for Emotional State Prediction. *Biomed. Signal Process. Control.* **2019**, *52*, 152–161. [CrossRef]
32. Mert, A.; Akan, A. Emotion Recognition Based on Time–Frequency Distribution of EEG Signals Using Multivariate Synchrosqueezing Transform. *Digit. Signal Process.* **2018**, *81*, 106–115. [CrossRef]
33. Jiang, X.; Xu, K.; Liu, X.; Dai, C.; Clifton, D.A.; Clancy, E.A.; Akay, M.; Chen, W. Neuromuscular Password-Based User Authentication. *IEEE Trans. Ind. Inform.* **2021**, *17*, 2641–2652. [CrossRef]
34. Gorur, K.; Bozkurt, M.R.; Bascil, M.S.; Temurtas, F. Comparative Evaluation for PCA and ICA on Tongue-Machine Interface Using Glossokinetic Potential Responses. *Celal Bayar Üniversitesi Fen Bilim. Derg.* **2020**, *16*, 35–46.
35. Zhao, H.; Chen, Y.; Pei, W.; Chen, H.; Wang, Y. Towards Online Applications of EEG Biometrics Using Visual Evoked Potentials. *Expert Syst. Appl.* **2021**, *177*, 114961. [CrossRef]
36. Paranjape, P.N.; Dhabu, M.M.; Deshpande, P.S.; Kekre, A.M. Cross-Correlation Aided Ensemble of Classifiers for BCI Oriented EEG Study. *IEEE Access* **2019**, *7*, 11985–11996. [CrossRef]
37. Fan, C.; Peng, Y.; Peng, S.; Zhang, H.; Wu, Y.; Kwong, S. Detection of Train Driver Fatigue and Distraction Based on Forehead EEG: A Time-Series Ensemble Learning Method. *IEEE Trans. Intell. Transp. Syst.* **2022**, *23*, 13559–13569. [CrossRef]
38. Lynn, H.M.; Pan, S.B.; Kim, P. A Deep Bidirectional GRU Network Model for Biometric Electrocardiogram Classification Based on Recurrent Neural Networks. *IEEE Access* **2019**, *7*, 145395–145405. [CrossRef]
39. Carrión-Ojeda, D.; Fonseca-Delgado, R.; Pineda, I. Analysis of Factors That Influence the Performance of Biometric Systems Based on EEG Signals. *Expert Syst. Appl.* **2021**, *165*, 113967. [CrossRef]
40. Gorur, K.; Olmez, E.; Ozer, Z.; Cetin, O. EEG-Driven Biometric Authentication for Investigation of Fourier Synchrosqueezed Transform-ICA Robust Framework. *Arab. J. Sci. Eng.* **2023**, *48*, 10901–10923. [CrossRef]
41. Dash, S.; Gajbhiye, P.; Sawangjai, P.; Sawadwuthikul, G.; Sudhawiyangkul, T.; Tripathy, R.K.; Pachori, R.B. Dyadic Boundary Points Based Empirical Wavelet Transform for the Elimination of Eye Movement and Eye Blink-Based Ocular Artifacts from EEG Signals. *Biomed. Signal Process. Control* **2023**, *85*, 104996. [CrossRef]
42. Coelli, S.; Medina Villalon, S.; Bonini, F.; Velmurugan, J.; López-Madrona, V.J.; Carron, R.; Bartolomei, F.; Badier, J.-M.; Bénar, C.-G. Comparison of Beamformer and ICA for Dynamic Connectivity Analysis: A Simultaneous MEG-SEEG Study. *Neuroimage* **2023**, *265*, 119806. [CrossRef]
43. Gonsisko, C.B.; Ferris, D.P.; Downey, R.J. ICanClean Improves Independent Component Analysis of Mobile Brain Imaging with EEG. *Sensors* **2023**, *23*, 928. [CrossRef] [PubMed]
44. Recurrence Plotting. Available online: <https://www.mathworks.com/matlabcentral/fileexchange/58246-tool-box-of-recurrence-plot-and-recurrence-quantification-analysis> (accessed on 7 July 2023).
45. Shalhaf, R.; Behnam, H.; Sleigh, J.W.; Steyn-Ross, D.A.; Steyn-Ross, M.L. Frontal-Temporal Synchronization of EEG Signals Quantified by Order Patterns Cross Recurrence Analysis During Propofol Anesthesia. *IEEE Trans. Neural Syst. Rehabil. Eng.* **2015**, *23*, 468–474. [CrossRef]
46. Ozer, I.; Cetin, O.; Gorur, K.; Temurtas, F. Improved Machine Learning Performances with Transfer Learning to Predicting Need for Hospitalization in Arboviral Infections against the Small Dataset. *Neural Comput. Appl.* **2021**, *33*, 14975–14989. [CrossRef] [PubMed]
47. Gorur, K.; Eraslan, B. The Single-Channel Dry Electrode SSVEP-Based Biometric Approach: Data Augmentation Techniques against Overfitting for RNN-Based Deep Models. *Phys. Eng. Sci. Med.* **2022**, *45*, 1219–1240. [CrossRef] [PubMed]
48. Ozer, I.; Ozer, C.K.; Karaca, A.C.; Gorur, K.; Kocak, I.; Cetin, O. Species-Level Microfossil Identification for Globotruncana Genus Using Hybrid Deep Learning Algorithms from the Scratch via a Low-Cost Light Microscope Imaging. *Multimed. Tools Appl.* **2023**, *82*, 13689–13718. [CrossRef]
49. Eraslan, B.; Gorur, K.; Temurtas, F. Novel Biometric Approach Based on Diaphragmatic Respiratory Movements Using Single-Lead EMG Signals. *IETE J. Res.* **2023**, 1–22. [CrossRef]
50. Ozer, I.; Efe, S.B.; Ozbay, H. A Combined Deep Learning Application for Short Term Load Forecasting. *Alex. Eng. J.* **2021**, *60*, 3807–3818. [CrossRef]
51. Kiliçarslan, S.; Közkurt, C.; Baş, S.; Elen, A. Detection and Classification of Pneumonia Using Novel Superior Exponential (SupEx) Activation Function in Convolutional Neural Networks. *Expert Syst. Appl.* **2023**, *217*, 119503. [CrossRef]
52. Haq, I.; Mazhar, T.; Malik, M.A.; Kamal, M.M.; Ullah, I.; Kim, T.; Hamdi, M.; Hamam, H. Lung Nodules Localization and Report Analysis from Computerized Tomography (CT) Scan Using a Novel Machine Learning Approach. *Appl. Sci.* **2022**, *12*, 12614. [CrossRef]
53. Kaushik, H.; Singh, D.; Kaur, M.; Alshazly, H.; Zaguia, A.; Hamam, H. Diabetic Retinopathy Diagnosis From Fundus Images Using Stacked Generalization of Deep Models. *IEEE Access* **2021**, *9*, 108276–108292. [CrossRef]
54. Zhao, H.; Wang, Y.; Liu, Z.; Pei, W.; Chen, H. Individual Identification Based on Code-Modulated Visual-Evoked Potentials. *IEEE Trans. Inf. Forensics Secur.* **2019**, *14*, 3206–3216. [CrossRef]

55. Wilaiprasitporn, T.; Dittthaporn, A.; Matchaparn, K.; Tongbuasirilai, T.; Banluesombatkul, N.; Chuangsuwanich, E. Affective EEG-Based Person Identification Using the Deep Learning Approach. *IEEE Trans. Cogn. Dev. Syst.* **2020**, *12*, 486–496. [[CrossRef](#)]
56. Maiorana, E. Deep Learning for EEG-Based Biometric Recognition. *Neurocomputing* **2020**, *410*, 374–386. [[CrossRef](#)]
57. Chakladar, D.D.; Kumar, P.; Roy, P.P.; Dogra, D.P.; Scheme, E.; Chang, V. A Multimodal-Siamese Neural Network (MSNN) for Person Verification Using Signatures and EEG. *Inf. Fusion* **2021**, *71*, 17–27. [[CrossRef](#)]
58. Bidgoly, A.J.; Bidgoly, H.J.; Arezoumand, Z. Towards a Universal and Privacy Preserving EEG-Based Authentication System. *Sci. Rep.* **2022**, *12*, 2531. [[CrossRef](#)]
59. Haq, I.; Mazhar, T.; Nasir, Q.; Razzaq, S.; Mohsan, S.A.H.; Alsharif, M.H.; Alkahtani, H.K.; Aljarbouh, A.; Mostafa, S.M. Machine Vision Approach for Diagnosing Tuberculosis (TB) Based on Computerized Tomography (CT) Scan Images. *Symmetry* **2022**, *14*, 1997. [[CrossRef](#)]
60. Pradeep Kumar, G.; Dutta, U.; Sharma, K.; Ganesan, R.A. EEG-Based Biometrics: Phase-Locking Value from Gamma Band Performs Well across Heterogeneous Datasets. In Proceedings of the 2022 International Conference of the Biometrics Special Interest Group (BIOSIG), Darmstadt, Germany, 14–16 September 2022; pp. 1–6.
61. Yu, X.; Aziz, M.Z.; Sadiq, M.T.; Jia, K.; Fan, Z.; Xiao, G. Computerized Multidomain EEG Classification System: A New Paradigm. *IEEE J. Biomed. Health Inform.* **2022**, *26*, 3626–3637. [[CrossRef](#)] [[PubMed](#)]
62. Varugeese, A.; Shahina, A.; Nawas, K.; Khan, A.N. EarNet: Biometric Embeddings for End to End Person Authentication System Using Transient Evoked Otoacoustic Emission Signals. *Neural Process. Lett.* **2022**, *54*, 21–41. [[CrossRef](#)]
63. Ahmed, F.; Bari, A.S.M.H.; Gavrilova, M.L. Emotion Recognition From Body Movement. *IEEE Access* **2020**, *8*, 11761–11781. [[CrossRef](#)]
64. Banerjee, A.; Datta, S.; Pal, M.; Konar, A.; Tibarewala, D.N.; Janarthanan, R. Classifying Electrooculogram to Detect Directional Eye Movements. *Procedia Technol.* **2013**, *10*, 67–75. [[CrossRef](#)]
65. Brain Mapping Plotting. Available online: <https://www.mathworks.com/matlabcentral/fileexchange/72729-topographic-eeg-meg-plot> (accessed on 10 July 2023).
66. Circular Graph Plotting. Available online: <https://www.mathworks.com/matlabcentral/fileexchange/48576-circulargraph> (accessed on 11 July 2023).
67. Zhao, Y.; Zhao, Y.; Durongbhan, P.; Chen, L.; Liu, J.; Billings, S.A.; Zis, P.; Unwin, Z.C.; De Marco, M.; Venneri, A.; et al. Imaging of Nonlinear and Dynamic Functional Brain Connectivity Based on EEG Recordings With the Application on the Diagnosis of Alzheimer’s Disease. *IEEE Trans. Med. Imaging* **2020**, *39*, 1571–1581. [[CrossRef](#)] [[PubMed](#)]
68. Cao, J.; Zhao, Y.; Shan, X.; Wei, H.; Guo, Y.; Chen, L.; Erkoyuncu, J.A.; Sarrigiannis, P.G. Brain Functional and Effective Connectivity Based on Electroencephalography Recordings: A Review. *Hum. Brain Mapp.* **2022**, *43*, 860–879. [[CrossRef](#)] [[PubMed](#)]
69. Guarino, A.; Malandrino, D.; Zaccagnino, R.; Capo, C.; Lettieri, N. Touchscreen Gestures as Images. A Transfer Learning Approach for Soft Biometric Traits Recognition. *Expert Syst. Appl.* **2023**, *219*, 119614. [[CrossRef](#)]
70. Chowdhury, D.P.; Bakshi, S.; Pero, C.; Olague, G.; Sa, P.K. Privacy Preserving Ear Recognition System Using Transfer Learning in Industry 4.0. *IEEE Trans. Ind. Inform.* **2023**, *19*, 6408–6417. [[CrossRef](#)]
71. Muhammad Hussain, N.; Rehman, A.U.; Othman, M.T.B.; Zafar, J.; Zafar, H.; Hamam, H. Accessing Artificial Intelligence for Fetus Health Status Using Hybrid Deep Learning Algorithm (AlexNet-SVM) on Cardiotocographic Data. *Sensors* **2022**, *22*, 5103. [[CrossRef](#)]
72. Mazhar, T.; Nasir, Q.; Haq, I.; Kamal, M.M.; Ullah, I.; Kim, T.; Mohamed, H.G.; Alwadai, N. A Novel Expert System for the Diagnosis and Treatment of Heart Disease. *Electronics* **2022**, *11*, 3989. [[CrossRef](#)]

Disclaimer/Publisher’s Note: The statements, opinions and data contained in all publications are solely those of the individual author(s) and contributor(s) and not of MDPI and/or the editor(s). MDPI and/or the editor(s) disclaim responsibility for any injury to people or property resulting from any ideas, methods, instructions or products referred to in the content.